Salt tolerance at single cell level in giant-celled Characeae

Mary J. Beilby*

Plant Membrane Biophysics, Physics/Biophysics, School of Physics, University of New South Wales, Sydney, NSW, Australia
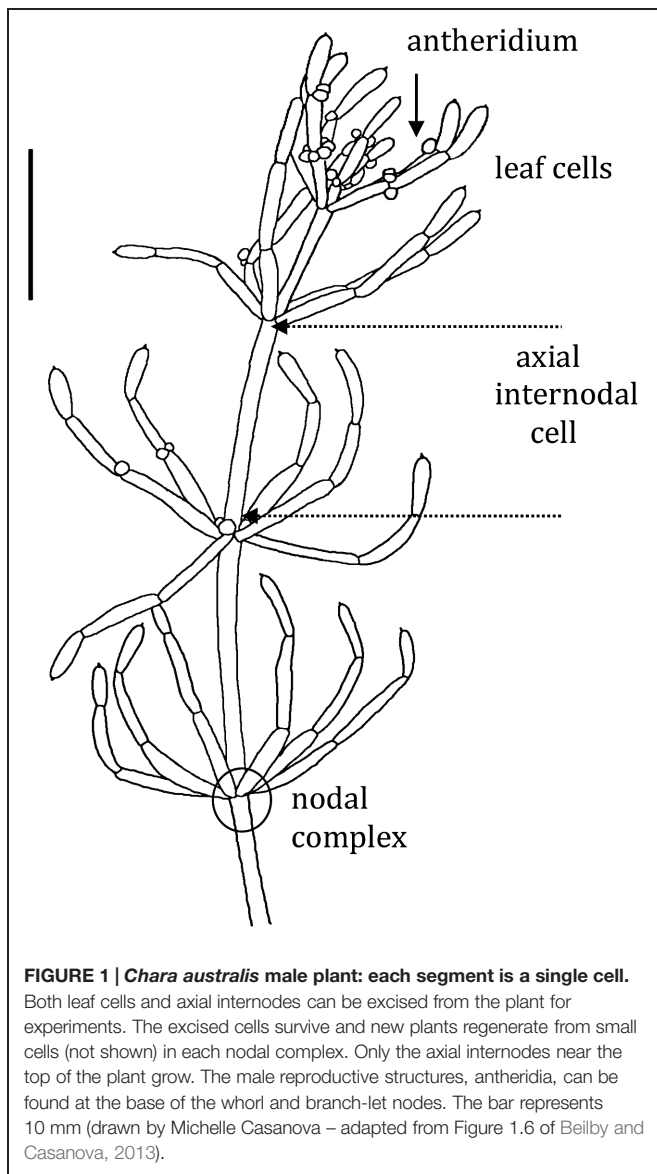
Characean plants provide an excellent experimental system for electrophysiology and physiology due to: (i) very large cell size, (ii) position on phylogenetic tree near the origin of land plants and (iii) continuous spectrum from very salt sensitive to very salt tolerant species. A range of experimental techniques is described, some unique to characean plants. Application of these methods provided electrical characteristics of membrane transporters, which dominate the membrane conductance under different outside conditions. With this considerable background knowledge the electrophysiology of salt sensitive and salt tolerant genera can be compared under salt and/or osmotic stress. Both salt tolerant and salt sensitive Characeae show a rise in membrane conductance and simultaneous increase in Na^+ influx upon exposure to saline medium. Salt tolerant *Chara longifolia* and *Lamprothamnium* sp. exhibit proton pump stimulation upon both turgor decrease and salinity increase, allowing the membrane PD to remain negative. The turgor is regulated through the inward K^+ rectifier and $2H^+/Cl^-$ symporter. *Lamprothamnium* plants can survive in hypersaline media up to twice seawater strength and withstand large sudden changes in salinity. Salt sensitive *C. australis* succumbs to 50–100 mM NaCl in few days. Cells exhibit no pump stimulation upon turgor decrease and at best transient pump stimulation upon salinity increase. Turgor is not regulated. The membrane PD exhibits characteristic noise upon exposure to salinity. Depolarization of membrane PD to excitation threshold sets off trains of action potentials, leading to further loses of K^+ and Cl^-. In final stages of salt damage the H^+/OH^- channels are thought to become the dominant transporter, dissipating the proton gradient and bringing the cell PD close to 0. The differences in transporter electrophysiology and their synergy under osmotic and/or saline stress in salt sensitive and salt tolerant characean cells are discussed in detail.

Keywords: Characeae, salt tolerance, electrophysiology, current-voltage characteristics, action potentials, proton pump, H^+/OH^- channels, non-selective cation channels

Introduction

Advantages of Characeae Experimental System for Salinity Studies
Large Cell Size and Simple Morphology

The thallus of characeaen plant consists of stems (axes), which are made of long multinucleate single cells interrupted by multicellular nodes. The nodes also give rise to branch-lets, which are similar to leaves of higher plants, but also consist of single cells (see **Figure 1**). The axial internode cell can be up to 1 mm in diameter and several cm long. The plants have colorless

FIGURE 1 | *Chara australis* male plant: each segment is a single cell.
Both leaf cells and axial internodes can be excised from the plant for
experiments. The excised cells survive and new plants regenerate from small
cells (not shown) in each nodal complex. Only the axial internodes near the
top of the plant grow. The male reproductive structures, antheridia, can be
found at the base of the whorl and branch-let nodes. The bar represents
10 mm (drawn by Michelle Casanova – adapted from Figure 1.6 of Beilby and
Casanova, 2013).

rhizoids instead of roots and these are also large cells joined
end to end. The axial or leaf cells survive excision from
the plant and can regenerate new plants from the adjacent
nodal complexes. These excised cells can be used in prolonged
experiments (up to 24 h). Pioneering electrical and trans-
port measurements were performed on the characean plants
(Walker, 1955; Hope and Walker, 1975; Beilby and Casanova,
2013).

Position on Phylogenetic Tree

Recent phylogenetic studies (Karol et al., 2001) have shown
that charophytes (that contain the Characeae family) are the
closest living relatives of the ancestors of all land plants. Land
plants emerged onto land ~470 million years ago (Domozych
et al., 2012), altering the atmosphere, reshaping the geology and
enabling the evolution of terrestrial animals (Sorensen et al.,
2010). While Characeae are now thought to be less closely related

to land plants than another charophyte group Zygnematales
(Wodniok et al., 2011; Timme et al., 2012), they are still posi-
tioned at the origin of land plants. Consequently, the large body
of electrophysiological and physiological data provides valuable
insights into many aspects of higher plants and into plant evolu-
tion (Beilby and Casanova, 2013). The question whether common
ancestors of Characeae and land plants lived in freshwater or
marine environments remains open (Graham and Gray, 2001;
Kelman et al., 2004) as characean fossils were found in sedi-
ments from brackish and marine habitats (Martin et al., 2003).
The transition of plants to land would have been less challenging
from freshwater, as marine algae would have faced desiccation
in air as well as hypersalinity in drying saline pools (Raven and
Edwards, 2001). Further, fresh water plants would have already
developed roots/rhizoids to acquire nutrients from the soil in
the oligotrophic environment (Rodriguez-Navarro and Rubio,
2006).

Salt Tolerant and Salt Sensitive Genera

The salt tolerance or sensitivity of the extant Characeae mirrors
that of land plant glycophyte–halophyte distribution: majority
live in fresh water and only few species are truly salt toler-
ant. The salt tolerant Characeae include some *Tolypella*, some
Chara, and all *Lamprothamnium* species. The most salt tolerant
species respond to salinity changes by complete turgor regulation
through changing vacuolar concentrations of K^+, Cl^- and some-
times Na^+ or sucrose: *Tolypella nidifica* and *glomerata* (Winter
et al., 1996), *Chara longifolia* (Hoffmann and Bisson, 1986), and
all *Lamprothamnium* species (Bisson and Kirst, 1980a; Okazaki
et al., 1984; Beilby et al., 1999; Casanova, 2013; Torn et al., 2014).
The salt tolerance of *Lamprothamnium* is remarkable: plants
with reproductive organs were found in Australian lakes at up
to twice the salinity of seawater (Burne et al., 1980; Williams,
1998). *C. australis* or *corallina* and *Nitella flexilis*, on the other
hand, are obligate freshwater species that regulate their internal
osmotic pressure (Gutknecht et al., 1978; Sanders, 1981; Bisson
and Bartholomew, 1984). *C. australis* plants exhibit 100% mortal-
ity after ~5 days in media containing 100 mM NaCl and 0.1 mM
Ca^{2+} (Shepherd et al., 2008).

Components of saline stress

To resolve different components of salinity stress, cells can be
exposed to a step up in osmolarity by employing sorbitol medium
(for instance), followed by isotonic saline solution. Such exper-
iments facilitate the measurement of short term defensive and
stress responses to each component in dose dependent manner.
The interpretation of results must allow for long term effects that
might be due to slow acting mechanisms, such as compatible
solute production and gene expression. For instance, Kanesaki
et al. (2002) found that salt stress and hyperosmotic stress
resulted in different gene expression in the ancient cyanobacteria
Synechocystis.

The osmotic stress and Na^+ toxicity require different types
of sensors and defensive mechanisms. The increase in osmo-
larity of the outside medium decreases the water potential and
water flows out of the cell within seconds of exposure (Steudle
and Zimmermann, 1974). The turgor of the cell drops, limiting

growth, making cells prone to injury and affecting photosynthetic activity (Allakhverdiev et al., 2000; Allakhverdiev and Murata, 2008). To control turgor, cells have to be able to sense it. The turgor sensors are still being identified (Boudsocq and Lauriere, 2005).

The increase in NaCl concentration presents another problem. Characean cells are not very permeable to Cl^-, but Na^+ rapidly floods the cells through non-selective cation channels (NSCCs; Demidchik and Maathuis, 2007). Cell has to expend energy to move Na^+ from the cytoplasm, where it replaces K^+ and inhibits metabolic functions. In cyanobacteria *Synechococcus* increased Na^+ medium concentration caused slow and irreversible inactivation of the photosystems (Allakhverdiev et al., 2000).

The Characeae plants are totally submerged in the medium and cannot fight salinity by forming salt glands or exporting salt to sacrificial tissues, or blocking salt movement into the shoot: every single cell in the plant has to be salt tolerant. Thus, comparing the electrophysiology of salt tolerant and salt sensitive characean species is likely to identify a minimal ensemble of factors that bestow salt tolerance at cellular level. This review reports on the progress of such studies.

Experimental Techniques

Characeae experimental system is unique by providing the comparison between the intact cell and the preparations with escalating interventions. The methodology adapted to these large celled plants is briefly summarized below.

The cytoplasmic layer of a single cell is up to 10 μm thick and the vacuole occupies 95% of the cell volume (Raven, 1987; Beilby and Shepherd, 1989). Microelectrodes can be positioned in the cytoplasm as well as in the vacuole, and membrane potential difference (PD) is measured separately across plasma membrane and tonoplast (Findlay and Hope, 1964; Beilby, 1989). However, the cytoplasm often excludes microelectrodes (Walker, 1955) and the cells become more prone to damage upon electrode re-insertion. The access to the cytoplasmic compartment can be improved by gentle centrifugation that moves cytoplasm to one end of the internode (Hirono and Mitsui, 1981; Beilby and Shepherd, 1989). The electrode is impaled before the streaming cytoplasm redistributes along the cell, or the cell can be wilted in the air and the cytoplasmic plug tied off, preparing cytoplasm-enriched fragments (Hirono and Mitsui, 1981; Beilby and Shepherd, 1989). Alternatively, cell ends can be cut and perfusion medium replaces the vacuolar sap (Tazawa, 1964). Rapid perfusion rate or inclusion of EGTA in the perfusion medium disintegrates the tonoplast (Williamson, 1975; Tazawa et al., 1976). This preparation not only makes the plasma membrane accessible, but also surrounds it with media of known composition. To study the tonoplast the plasma membrane is permeabilized using EGTA (Shimmen and Tazawa, 1982; Tester et al., 1987). The tonoplast also surrounds cytoplasmic droplets formed by cutting an internodal cell and immersing the end in vacuolar sap like medium (Luhring, 1986). While some of the latter techniques

allow experimenters greater control over the surroundings of each membrane, they also perturb the living cell and may introduce artifacts.

The size of characean cells facilitated early water permeability measurements (Wayne and Tazawa, 1990), using transcellular osmosis technique. The internodal cell was placed in two-compartment chamber with media of different osmolarity in each chamber. The reversible partial block by mercury derivatives suggested that some of the water moves across the membrane through water channels aquaporins. Pressure probe single cell measurements confirmed presence of aquaporins, although fraction of water and uncharged solutes permeating through them (as opposed to lipid bilayer) is still under consideration (Henzler and Steudle, 1995; Schutz and Tyerman, 1997). Ye et al. (2004, 2005) formulated tension/cohesion model for closure of water channels with increasing osmolarity. Henzler et al. (2004) found that water channels also close in response to oxidative stress.

The size of the cells can be a disadvantage when the membrane PD is controlled by voltage clamp. A longitudinal wire electrode or a small central compartment in a multi-compartment cell holder may be employed to space clamp the cell: to pass uniform currents and avoid conductance "hot spots" (Smith, 1984a; Beilby, 1990). To obtain current-voltage (I/V) characteristics of the plasma membrane (or both membranes in series), the membrane PD is clamped to bipolar staircase (Gradmann et al., 1978). The alternating short excursions to PD levels above and below the resting PD avoid prolonged large currents and transport number effects (accumulation of ions near the membrane outer surface – see Beilby, 1990). I/V profiles over wide PD windows (up to 500 mV) can be obtained in less than 10 s (Beilby, 1989). However, it is necessary to check the raw data to insure that the current has leveled at the end of each pulse and that it returned to near zero while the membrane PD was clamped at the resting level. Long time current dependencies need to be investigated separately by prolonged (seconds) voltage clamp to different PD levels.

Background of Characeae Electrophysiology

Thousands of I/V profiles have now been recorded on various Characeae species and under a range of conditions. The results are mostly consistent, suggesting that the plasma membrane can take on different states, depending on the outside conditions. This large body of data allows identification of ion transporter I/V profiles, their responses and synergies at the time of abiotic stress (such as salinity increase), as well as comparison to transporters of higher plants. The forthcoming sequencing of Characeae (Stefan Rensing, personal communication) will allow even more detailed comparisons on molecular level.

There are many ion transporters in both plasma membrane and the tonoplast and new ones are being discovered. However, only a small number of transporter types dominate the membrane conductance and the I/V profiles. The I/V characteristics can change substantially depending on the pH and K^+

concentration of the outside medium (see the central part of **Figure 2**).

Pump State

At neutral to slightly alkaline pH_o with K^+ below 1 mM (a typical fresh water pond, where majority of characean species live), the plasma membrane resting PD is quite negative at

-200 to -250 mV. The I/V characteristics exhibit a beautiful sigmoid shape generated by the energizing export of protons from the cytoplasm by the proton ATPase (see the bottom part of **Figure 2** and **Figure 3**). For history of the characean proton pump research and modeling with the cyclic enzyme-mediated HGSS model (Hansen et al., 1981) see chapter 2 of Beilby and Casanova (2013).
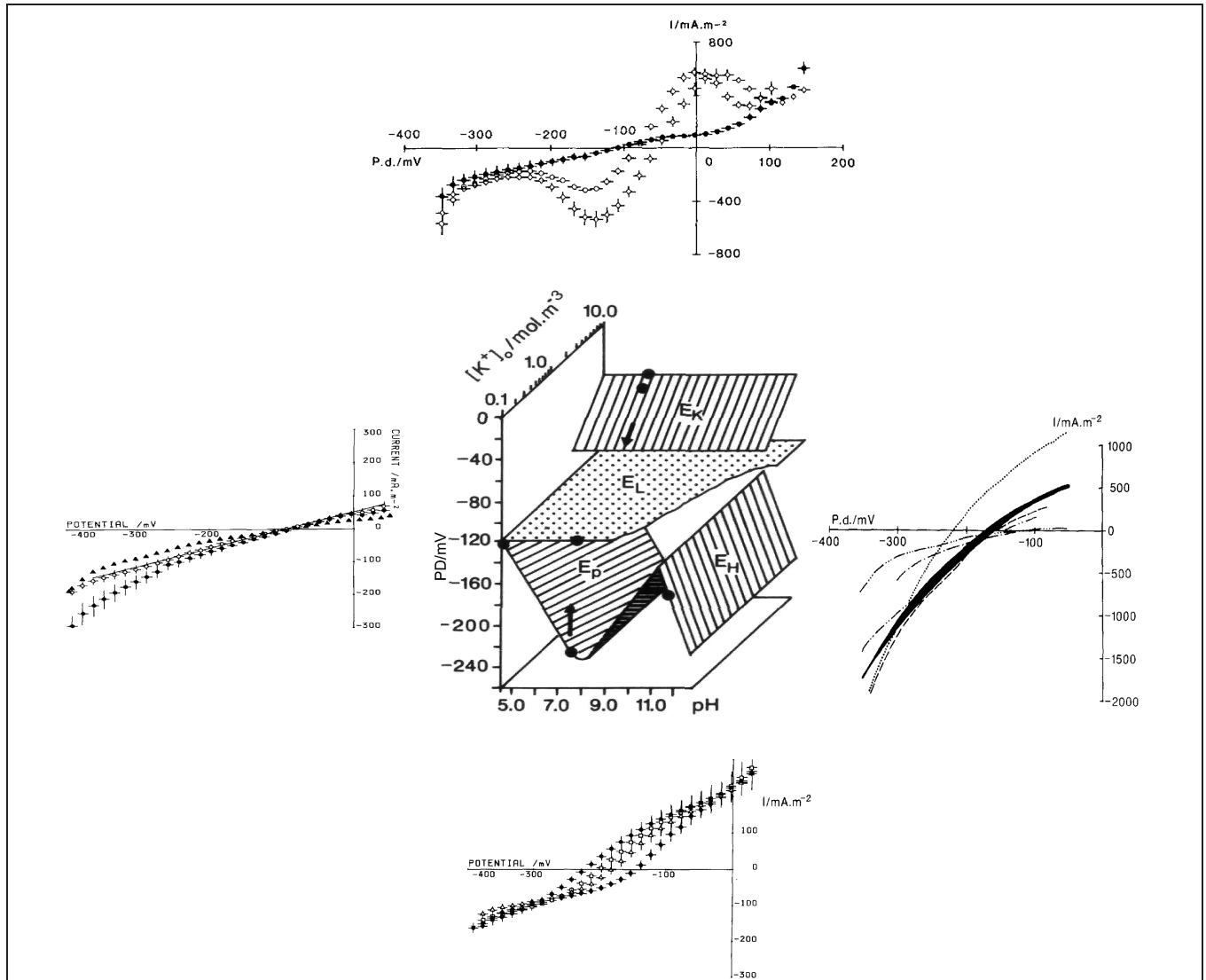

FIGURE 2 | Different states of plasma membrane: central panel shows the membrane PD in different states as function of pH_o and $[K^+]_o$ (E_p reversal PD of the proton pump, E_L reversal PD for the background/leak current, E_K Nernst PD for K^+, E_H Nernst PD for H^+ or OH^-). The figure is based on **Figure 1** (Beilby, 1990) with the I/V characteristics updated from later publications. Bottom panel: proton pump-dominated state at pH_o of 4.5 ♦, 5.5 ▲, 6.5 □, and 7.5 ● (Beilby, 1984). E_p is most negative at pH_o 7–8 (shown as a dot on the "pump surface") and tends toward E_L at pH 4.5 (a point where the pump and background surfaces meet). Left panel: background state with 10 I/V runs summarized from nine cells exposed to DES (diethyl stilbestrol). These cells stabilized after 30 min DES exposure (shown by a point on the background surface). Four La^{3+}-treated cells exposed to DES for 30 min, ●, continued to change as shown by a single I/V run on La^{3+}-treated cell, with DES exposure of

1 hr 15 min (Beilby, 1984). Top panel (Beilby, 1986): I/V characteristics of cells in K^+ state, summary from seven cells in 5 mM K^+ APW ○, 10 mM K^+ APW ◇ (the two points on K^+ surface) and 0.1 mM K^+ APW ● (here the K^+ channels closed revealing the background state, see the arrow in central part of figure). Right panel (Beilby and Bisson, 1992): high pH state: pH 11.5 (dotted line), pH 10.5 – two I/V runs in fast succession shown by black shading, pH 10.5 + 2.5 mM Na_2SO_4 (dashed line), back to pH 10.5 (dash, two dots, dash line), pH 10.5 + 10 mM Na_2SO_4 (dash dot dash line), and finally back to pH 10.5 (dash, three dots, dash line). The I/V characteristics in this state can be quite variable. As NaOH (5–30 mM) was used to bring the APW to high pH, the effect of Na^+ concentration increase was explored. Beilby and Bisson (1992) did not find a consistent effect, but high concentrations might affect the H^+/OH^- channel activation via ROS response, see text.
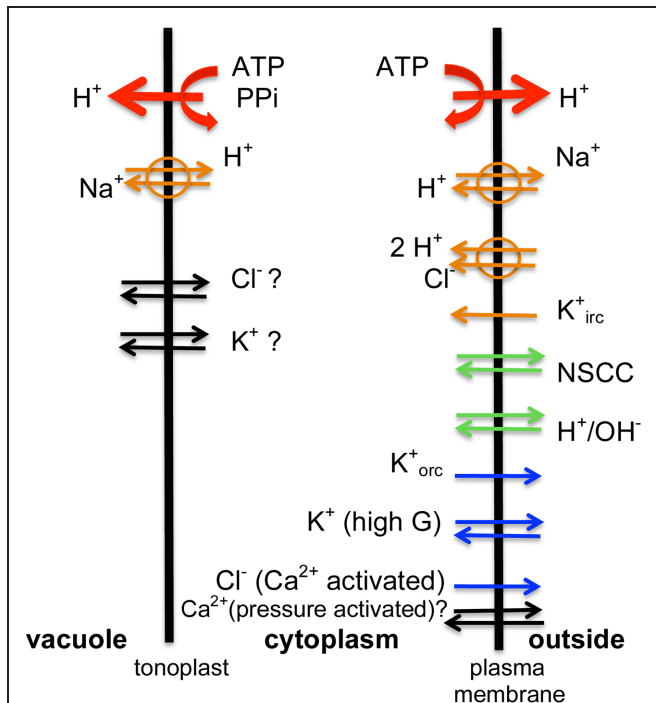
FIGURE 3 | The transporter scheme for the characean cell: same types of transporters are found in both salt tolerant and salt sensitive genera. The energizing ATPases and PPases (red arrows) drive H$^+$ out of the cytoplasm. The proton motive force is employed by Na$^+$/H$^+$ aniporters and 2H$^+$/Cl$^-$ symporter, while negative PD opens K$^+$ inward rectifier (orange arrows). In salt sensitive Characeae the pumps are not stimulated by low turgor and fail in saline media. In normal pond water NSCC channels bring in nutrients and H$^+$/OH$^-$ channels aid photosynthesis by exporting OH$^-$ in alkaline bands (green arrows). In time of saline stress Na$^+$ enters through NSCC channels in all Characeae, but salt tolerant Characeae keep the Na$^+$/H$^+$ antiporters going and prevent global opening of H$^+$/OH$^-$ channels. The outward rectifier, the high conductance K$^+$ channels or Ca^{2+} activated Cl$^-$ channels are not active in steady state (blue arrows). The inflow of Ca^{2+} into the cytoplasm (black arrows) at the time of AP or hypoosmotic regulation is well documented, but the sources (outside, internal stores in the cytoplasm or the vacuole) are still disputed and beyond the scope of this article. Similarly, there are K$^+$ and Cl$^-$ transporters on the tonoplast (black arrows), but discussion of these is beyond the scope of this article. The Ca^{2+}-activated Cl$^-$ channels provide the depolarizing phase of the AP with the outward rectifier contributing to the recovery of resting PD. In salt tolerant Characeae the Ca^{2+}-activated Cl$^-$ channels and high conductance K$^+$ channels mediate hypoosmotic regulation.

Background State

If the pump is turned off by some metabolic inhibitors or by circadian rhythms, the underlying null or background state is revealed: more depolarized resting PD near −100 mV and linear I/V profile in the PD window of ∼ +50 to ∼ −350 mV (see the left part of **Figure 2**). The background current was fitted by an empirical equation:

$$I_{background} = G_{background}(V - E_{background})$$

where $G_{background}$ is PD independent conductance and $E_{background}$ (E_L in **Figure 2**) is the reversal PD chosen as

−100 (± 20) mV (−120 mV in **Figure 2**). This value was derived experimentally and its origin is still a puzzle. The background current is thought to flow through non-selective PD-independent cation channels (NSCC – Demidchik and Maathuis, 2007), which supply micronutrients to the plant and contribute to signaling (**Figure 3**).

At PD levels more negative than ∼ −300 mV the background current is obscured by the inward rectifier current, K^+_{irc}, while at PD levels more positive than ∼ −50 mV the outward rectifier current, K^+_{orc}, predominates. The inward and outward rectifier currents, mainly carried by K$^+$, were modeled by the Goldman-Hodgkin-Katz (GHK) equation, multiplied by the Boltzmann distribution of open probabilities to make the PD-dependence stronger (Beilby and Walker, 1996; Amtmann and Sanders, 1999). The early activation of inward rectifier K^+_{irc} can be observed near −400 mV on the pump state curves (bottom of **Figure 2**) and K$^+$ state curves (top of **Figure 2**). The early activation of outward rectifier, K^+_{orc}, can be found near 0 PD in pump state curves and at +50 mV in the K$^+$ State curves.

The pump state and the underlaying background state are the native states for the salt sensitive Characeae in their low salt, slightly alkaline pond media.

K$^+$ State

As K$^+$ concentration in the medium rises above ∼1 mM, large conductance K$^+$ (high G K$^+$) channels open, short-circuit the pump current and become the dominant membrane conductance (Oda, 1962; Smith and Walker, 1981; Sokolik and Yurin, 1981; Keifer and Lucas, 1982; Smith, 1984b; Beilby, 1985; Sokolik and Yurin, 1986; Tester, 1988a,b,c). The I/V characteristics of the K$^+$ state are very distinct: the two regions of negative conductance arise from the strong PD dependence of the channels (see the top part of **Figure 2**). The I/V profiles can also be modeled by GHK equation supplemented with Boltzmann distribution of open probabilities (Beilby and Shepherd, 2001b). The K$^+$ conductance increases with outside K$^+$ concentration until it becomes so large that the cells cannot be voltage-clamped. This property of K$^+$ state is exploited in K$^+$ anesthesia technique of measuring membrane PD without inserted electrodes (Hayama et al., 1979). K$^+$ channels are blocked totally and reversibly by tetraethylammonium (TEA) revealing the linear background state, which seems independent of K$^+$ concentration (see the top part of **Figure 2**). The activation of high G K$^+$ channels is observed in tissues, stomata and roots of land plants (Epstein, 1976; Cheeseman and Hanson, 1979; Blatt, 1988).

High pH State

If pH of the medium rises above 9.0, the resting PD starts to follow the equilibrium PD for H$^+$ or OH$^-$ with resting PD more negative than −200 mV in some cells (Bisson and Walker, 1980). The membrane conductance can increase by up to 5 S.m^{-2}. This H$^+$/OH$^-$ state is inhibited by darkness, photosynthesis inhibitor DCMU, various metabolic inhibitors (such as DES or DCCD) or lack of Ca^{2+} in the medium, which can be replaced by Mg^{2+} (Bisson, 1984). Beilby and Bisson (1992) found that the I/V characteristics exhibit slight downward curvature (see right part of **Figure 2**). However, the conductance and the reversal PD

are quite variable. Al Khazaaly and Beilby (2012) modeled the I/V characteristics at high pH, using the GHK equation supplemented by the Boltzmann probability distribution. H^+ or OH^- was tested as the transported ion: OH^- seems more probable, as the channel number multiplied by the channel conductance remains relatively constant throughout the pH range, whereas for H^+ the same parameter had to be increased by several orders of magnitude to match the high conductance at very high pH (Beilby and Casanova, 2013). The high pH state is reversibly blocked by the zinc ion, potent inhibitor of animal H^+ channels (Al Khazaaly and Beilby, 2012). The H^+/OH^- channels participate in the pH banding pattern, where ring shaped zones of pump-dominated or H^+/OH^- channel dominated membrane are set up by the cells to acquire DIC (dissolved inorganic carbon) and make photosynthesis more efficient (Hope and Walker, 1975; Beilby and Bisson, 2012; Beilby and Casanova, 2013).

In their normal habitats, the whole Characeae cells and plants are not exposed to pH of 10 and higher. However, due to export of OH^- in the alkaline bands, the external pH rises to 10 and above. The exposure of cells to high pH highlighted mechanisms leading to banding formation (Beilby and Bisson, 2012) and facilitated detailed description and modeling of the I/V characteristics of the H^+/OH^- channels (Beilby and Bisson, 1992; Beilby and Al Khazaaly, 2009; Al Khazaaly and Beilby, 2012).

A detailed study of the I/V characteristics of *Lamprothamnium* cells acclimated to salinities ranging from 0.2 to full artificial sea water (ASW) showed that in the higher salinities (from ~1/3 ASW) the cells could be found in three different resting states: pump state, background state or K^+ state (Beilby and Shepherd, 2001a). Similarly to salt sensitive *C. australis* (left side of **Figure 2**), *Lamprothamnium* cells in the background state exhibited near linear I/V characteristics between −50 and −200 mV with reversal PD close to −100 mV.

Surviving in Saline Media: Salt Tolerant Characeae

Hyperosmotic Adjustment Mechanisms

Upon increase of osmolarity in the external medium, the water potential drops, water flows out of the cell and the turgor pressure decreases. To restore turgor the osmolarity of the vacuole must be increased. This process requires energy. The energizing elements of the ion transport are proton ATPases and PPases on the plasma membrane and the tonoplast (**Figure 3**). The main osmotica, K^+ and Cl^-, are imported through inward rectifier K^+_{irc} and $2H^+/Cl^-$ symporter (**Figure 3**). Such turgor adjustment is well documented in higher plants (for instance in *Arabidopsis* roots – Shabala and Lew, 2002). The Na^+ inflow occurs through the NSCCs (Tester and Davenport, 2003; Demidchik and Maathuis, 2007). These channels can be partially blocked by high Ca^{2+} in the external medium (Tester and Davenport, 2003). The plant cells strive to keep low Na^+ in the cytoplasm employing Na^+/H^+ antiporters at both membranes (Tester and Davenport, 2003 and **Figure 3**). Several of these mechanisms were initially discovered in the Characeae experiments.
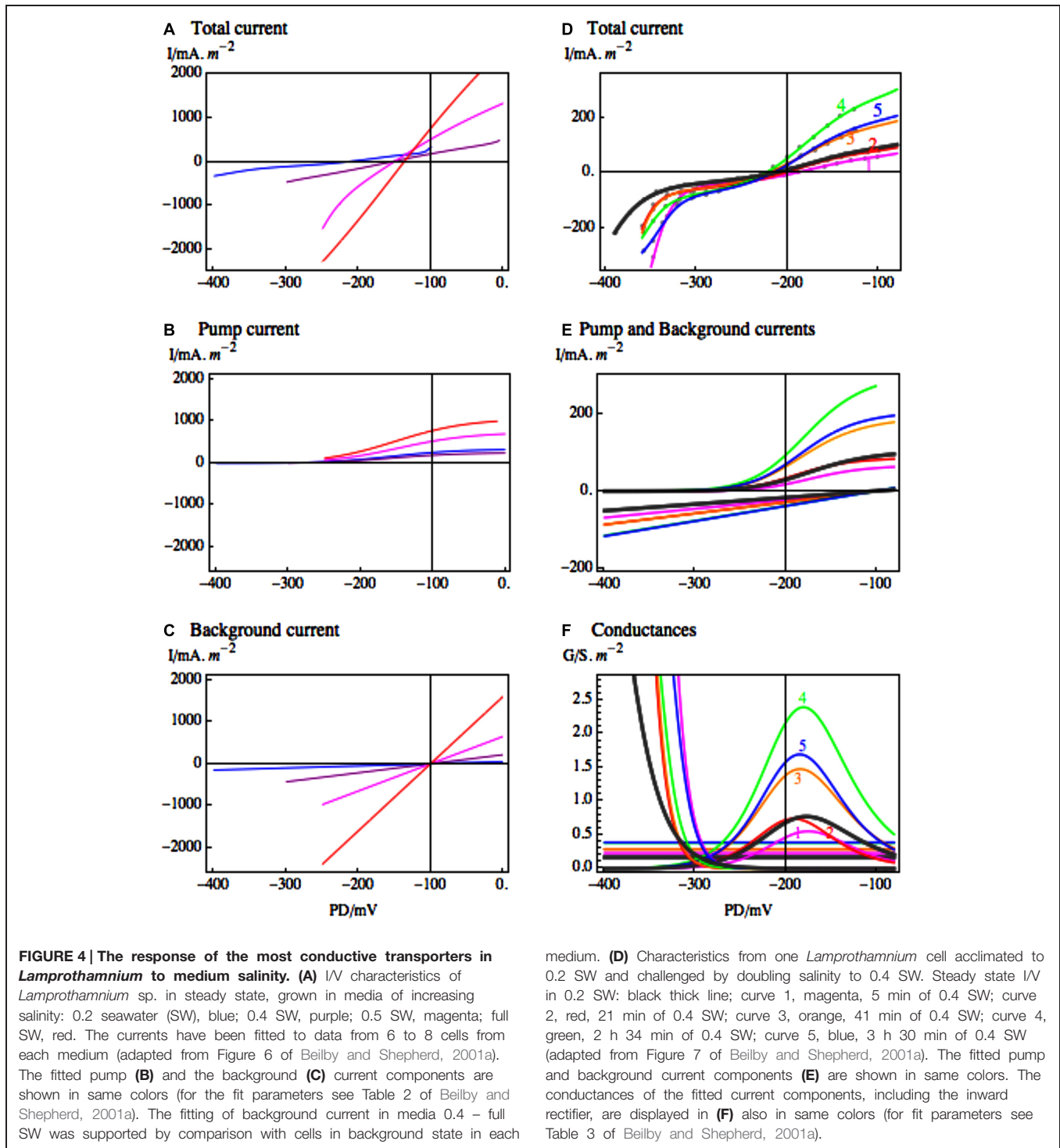
H^+ Pump Activation

Bisson and Kirst (1980a,b) and Okazaki et al. (1984) observed hyperpolarization of membrane PD in *Lamprothamnium* sp. upon increase in salinity while the vacuolar concentrations of K^+ and Cl^- increased to regulate turgor to ~300 mosmol/kg (Bisson and Kirst, 1980b). Reid et al. (1984) resolved the response further into a transient PD depolarization for ~10 min, followed by hyperpolarization. They also found a transient drop in ATP concentration paralleled by a rise in respiration. The cytoplasmic streaming speed diminished briefly and then increased, while the influxes of Na^+, K^+, and Cl^- increased over 800 min. Working on the only salt tolerant *Chara* species, *C. longifolia*, Yao et al. (1992) and Yao and Bisson (1993) demonstrated that the proton pumping also increased in more saline media and turgor was regulated: cell PD transiently hyperpolarized and conductance increased (95–144 h). Okazaki et al. (1984) challenged *Lamprothamnium* cells with a sorbitol hyperosmotic step and also observed membrane hyperpolarization. They suggested that it is the decrease in turgor, which initiates the turgor regulation observed by Bisson and Kirst (1980a). To confirm this hypothesis Al Khazaaly and Beilby (2007) compared the step from 1/6 ASW to 1/3 ASW in salinity and equivalent step in osmolarity using sorbitol (Sorbitol ASW). The I/V characteristics were measured for up to 7 h following either type of hyperosmotic step and the data were modeled to resolve the responses of various transporters. In both treatments the average cell PD hyperpolarized to similar level (~ −150 mV) through the activation of the proton pump and the inward rectifier channels were opened at more positive PDs. The authors also found that the cells in K^+ state were able to switch to pump state upon turgor decrease or salinity increase, and were able to regulate turgor.

Na^+ Transport

Kishimoto and Tazawa (1965), early pioneers of the I/V technique, measured increased *Lamprothamnium* cell membrane conductance with rising salinity of the medium. However, modeling of the currents through the different transporters was necessary to resolve the increase of pump conductance and the conductance due to Na^+ inflow. The *Lamprothamnium* cells in the background state showed clearly that the slope (conductance) of the $I_{background}$ increased with medium salinity, while $E_{background}$ remained close to −100 mV (Beilby and Shepherd, 2001a and **Figure 4C**). These cells confirmed the correct modeling of this underlying state for cells in pump state and K^+ state (Beilby and Shepherd, 2001a). Al Khazaaly and Beilby (2007) confirmed that after exposure to Sorbitol ASW the background conductance actually decreased slightly, while in 1/3 ASW the background conductance increased by about a third.

Working on *C. longifolia* the Bisson group found that the Na^+/Ca^{2+} ratio is important for turgor regulation (Hoffmann and Bisson, 1988; Hoffmann et al., 1989). The freshwater-incubated cells could only survive salinity increase and regulate turgor if the ratio was 10:1. Interestingly, the cells acclimated to their native medium (~100 mM Na^+ and 100 mM Mg^{2+} with Cl^- and SO_4^{2-} as main anions) did survive higher Na^+/Ca^{2+}

FIGURE 4 | The response of the most conductive transporters in *Lamprothamnium* to medium salinity. (A) I/V characteristics of *Lamprothamnium* sp. in steady state, grown in media of increasing salinity: 0.2 seawater (SW), blue; 0.4 SW, purple; 0.5 SW, magenta; full SW, red. The currents have been fitted to data from 6 to 8 cells from each medium (adapted from Figure 6 of Beilby and Shepherd, 2001a). The fitted pump **(B)** and the background **(C)** current components are shown in same colors (for the fit parameters see Table 2 of Beilby and Shepherd, 2001a). The fitting of background current in media 0.4 – full SW was supported by comparison with cells in background state in each medium. **(D)** Characteristics from one *Lamprothamnium* cell acclimated to 0.2 SW and challenged by doubling salinity to 0.4 SW. Steady state I/V in 0.2 SW: black thick line; curve 1, magenta, 5 min of 0.4 SW; curve 2, red, 21 min of 0.4 SW; curve 3, orange, 41 min of 0.4 SW; curve 4, green, 2 h 34 min of 0.4 SW; curve 5, blue, 3 h 30 min of 0.4 SW (adapted from Figure 7 of Beilby and Shepherd, 2001a). The fitted pump and background current components **(E)** are shown in same colors. The conductances of the fitted current components, including the inward rectifier, are displayed in **(F)** also in same colors (for fit parameters see Table 3 of Beilby and Shepherd, 2001a).

ratios. Higher Ca^{2+} in the medium partially blocks the NSCC channels and diminishes the Na^+ inflow.

Tester and Davenport (2003) estimated that cytoplasm would equalize with the external medium of 50 mM NaCl in 3 min, if there was no Na^+ efflux. To frustrate the electrophysiologist Na^+/H^+ antiporter is electrically silent and consequently independent of membrane PD.

Thermodynamically, the Na^+/H^+ anti-porter is an example of a Maxwell's demon. Protons are pumped out of the cytoplasm to create inward proton gradient and negative membrane PD, Na^+ flows in passively and is then removed by a "swap" for a proton. The primary energizing process is the proton pumping with ATP consumption as the cost to the cell (**Figure 3**).

Whittington and Bisson (1994) employed isotope $^{22}Na^+$ to measure Na^+ influx and efflux in salt sensitive *C. corallina* and fresh water-grown salt tolerant *C. longifolia* under mild salt stress of 20 mM NaCl. They found lower influx in salt tolerant *C. longifolia*. The addition of 1 mM Ca^{2+} to the medium greatly reduced influx into *C. corallina*. Na^+ efflux was greater in *C. longifolia* and increased in both Characeae as pH_o changed from 7 to 5. In both species the efflux was unchanged by pH increase from 7 to 9. The efflux was not significantly inhibited by the Na^+/K^+ pump inhibitor amiloride, confirming the absence of such pump. *C. longifolia* grown in native saline medium (130 mM Na^+ and 110 mM $MgSO_4$) exhibited greater Na^+ efflux, especially at pH_o 5 (Kiegle and Bisson, 1996). At pH 9 the calculated $\Delta\mu_H$ was not sufficient to drive the efflux and the authors concluded that there might be other mechanisms for Na^+ efflux.

Davenport et al. (1996) found that despite surviving in salinities at seawater level and above, *Lamprothamnium* is also dependent on Ca^{2+} concentration of the medium. At low Ca^{2+} Na^+ influx increased and the cells died. For both *Lamprothamnium* and *Chara australis* influx of $\sim$300 nmolm^{-3}s^{-1} seems to be the limiting level for survival. The authors showed convincingly that low turgor promotes greater Na^+ influx. Reduction of turgor by addition of up to 100 mM mannitol doubled the influx even at low medium concentration of 3.5 mM NaCl. Conversely, increasing the turgor of *Chara* cells by soaking them in concentrated KCl decreased the Na^+ influx.

Modeling Transporter Response to Salinity

Resolving the different transporter populations by modeling the I_{Total}/V characteristics provides quantitative estimates of response to salinity/osmolarity increase. In *Lamprothamnium* plants acclimated to range of salinities the conductance of the background state increased with salinity from 0.5 S.m^{-2} in 0.2 ASW to 22.0 S.m^{-2} in full ASW (see **Figure 4C**). The cells in pump state increased pump currents in more saline media (see **Figure 4B**) with conductance maxima at 2 S.m^{-2} in 0.2 ASW and 5 S.m^{-2} in full ASW. But even with greater proton pumping the cell resting PDs became more depolarized with rising salinity: below -200 mV in 0.2 ASW to $\sim$ -140 mV in full ASW (see **Figure 4A**). **Figures 4A–C** contain important message: *Lamprothamnium* cell can sense Na^+ concentration in the medium and adjust pump activity to counteract the increased background conductance. In higher salinity the cell has to expend more energy powering the proton pump. The cells in K^+ or background state could be "resting," saving energy temporarily, while the proton gradient runs down. Al Khazaaly and Beilby (2007) demonstrated that these cells are able to "switch" the pump back on. It might be interesting to find out if there is a periodic (perhaps circadian) pattern for the different states to dominate.

Beilby and Shepherd (2001a) also modeled transient changes of the *Lamprothamnium* proton pump after salinity step of 150 mOsmol.kg^{-1}, starting in dilute medium of 0.2 ASW (see **Figures 4D–F**). There was an initial decrease in the proton pump current and peak conductance (see **Figures 4D,E**, curve 1 magenta), coinciding with the low ATP concentration found by Reid et al. (1984). Then both the current and peak conductance

increased, coming to a maximum after $\sim$2 h of hyperosmotic challenge (see **Figures 4D,E**, curve 4, green). Inward rectifier current responded within minutes of salinity increase by activating at more positive PDs (**Figures 4D,F**).

Thus the more researched salt tolerant Characeae, *Lamprothamnium sp.* and *Chara longifolia*, both exhibit proton pump stimulation upon salinity increase to keep the membrane PD negative, despite partial short-circuit of greater background conductance of Na^+ inflow through NSCC channels. This response is crucial, as the proton pump provides the energy source for both up-regulation of turgor and prevention of toxic built up of Na^+ in the cytoplasm (**Figure 3**). The membrane PD more negative than E_K facilitates the import of K^+ through the inward rectifier channels to maintain K^+/Na^+ ratio supportive to normal enzyme function. K^+ is also transported into the vacuole for turgor regulation. The import of Cl^- into the vacuole upon salinity/osmolarity increase is mediated by the $2H^+/Cl^-$ symporter at plasma membrane, again powered by the proton electrochemical gradient (Sanders, 1980; Beilby and Walker, 1981). The Cl^- transporters at the tonoplast also have to work "uphill" to achieve the observed vacuolar concentrations (Teakle and Tyerman, 2010).

Hypoosmotic Adjustment Mechanisms

Plants living in saline media have to cope with salinity changes: osmolarity of a shallow pond can drop in minutes in a torrential downpour. Cells have been observed to explode if the turgor became too great. What are the mechanisms for such sudden downward turgor adjustment? Working with different starting media and different salinity/osmolarity decrease in *Lamprothamnium* or *C. longifolia,* several investigators found rapid membrane depolarization to $\sim$ -70 mV for 30–60 min, accompanied by conductance rise up to an order of magnitude, with subsequent partial repolarization (Reid et al., 1984; Okazaki et al., 1984; Hoffmann and Bisson, 1990; Okazaki and Iwasaki, 1992; Beilby and Shepherd, 1996).

Okazaki and Tazawa (1986a,b) also observed streaming inhibition for up to 20 min upon hypoosmotic challenge. Low Ca^{2+} medium or presence of Ca^{2+} antagonist nifedipine abolished the depolarization, conductance increase and turgor regulation. Okazaki and Tazawa (1987) visualized the Ca^{2+} increase in the cytoplasm using fluorescence techniques: in ASW with normal high Ca^{2+} content fluorescence increased after about 1 min of hypoosmotic stress. If the cell was given a hypoosmotic shock in low Ca^{2+} ASW and Ca^{2+} increased later, the fluorescence rose immediately. The authors concluded that turgor mediated opening of Ca^{2+} channels has a small delay. Okazaki et al. (2002) made more detailed measurements of Ca^{2+} concentration in *Lamprothamnium* under hypoosmotic stress. After initial rapid increase from resting value of 100 nM to peak of 600 nM, the concentration dropped at 0.9 nM/s. They also estimated that maximum conductance was reached by 300 nM, but 400–600 nM was necessary for cytoplasmic streaming cessation.
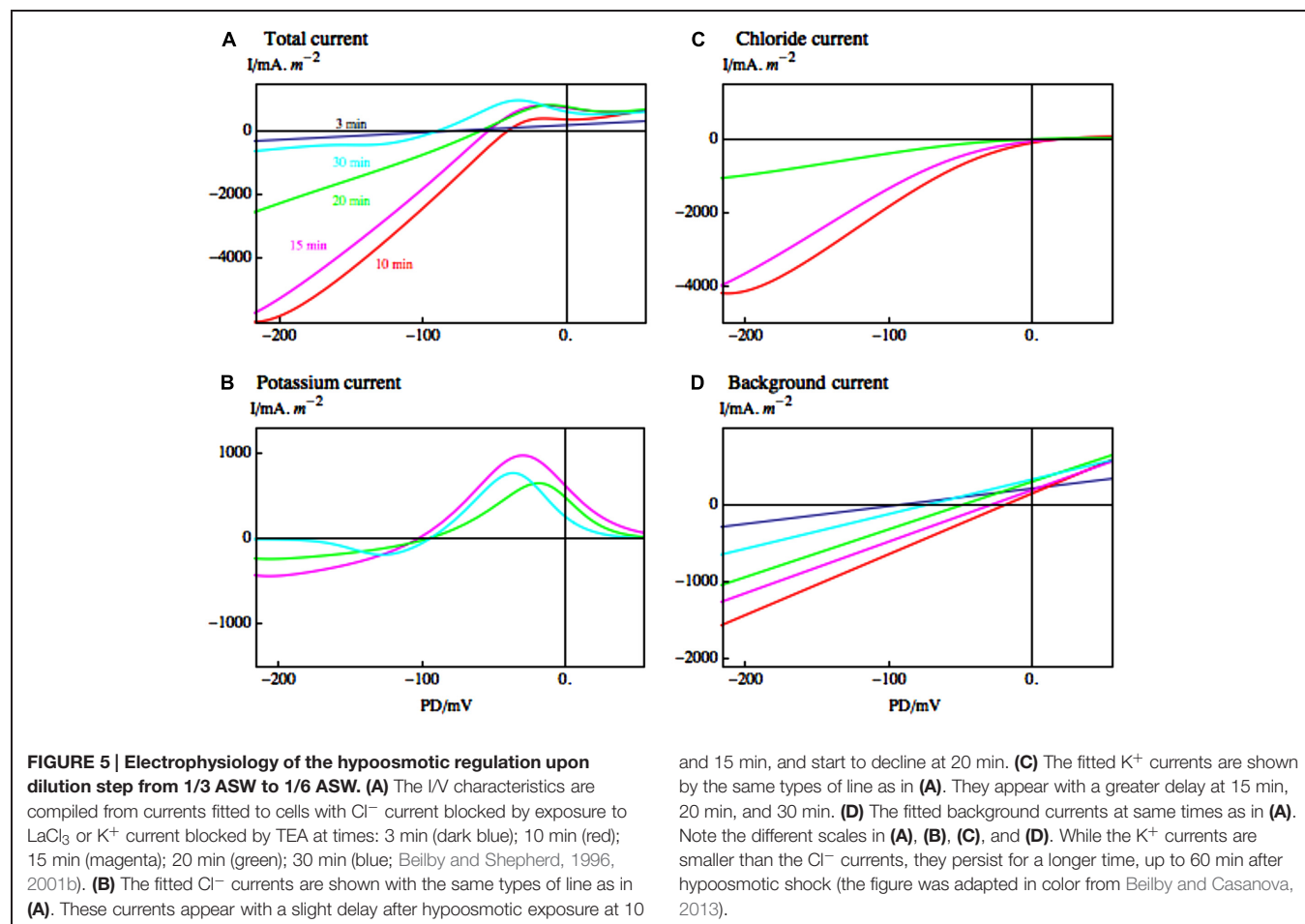
As turgor regulation in *Lamprothamnium* was mostly achieved by varying K^+ and Cl^- in the vacuole (Bisson and Kirst, 1980a), the increase of conductance must be due to the efflux of these ions. Okazaki and Iwasaki (1992) found

a good correlation between Cl^- efflux and rise in conductance. Beilby and Shepherd (1996) employed the I/V technique and pharmacological dissection (TEA or $LaCl_3$) to resolve the timing of the Cl^- and K^+ outflow (see **Figure 5**). The large G K^+ channels, identified by their typical I/V characteristics (compare top part of **Figures 2 and 5B**) and total block by TEA, mediate the K^+ outflow (Beilby and Shepherd, 2001b). The K^+ channel activation is clearly visible with the Cl^- currents blocked by La^{3+} (**Figure 5B**). The opening of K^+ channels is preceded by the Cl^- channel activation, but there is some overlap (Beilby and Shepherd, 1996). These results also suggest that K^+ channels do not require increased Ca^{2+} concentration in the cytoplasm. By Occam's razor argument the Cl^- channels are assumed to be the same Ca^{2+}-activated channels that participate in the AP (Beilby, 2007, see also **Figure 3**). With the Ca^{2+} concentration in the cytoplasm high for many minutes (Okazaki et al., 2002), the I/V characteristics of the Cl^- channels could be investigated (see **Figure 5C** and Beilby and Shepherd, 2006b). The channels are inwardly rectifying with maximum conductance near -100 mV and strong inactivation near 0 PD. Bisson et al. (1995) found that in *C. longifolia* K^+ channel activation preceded the Cl^- channel activation and that this second stage also required external Ca^{2+}.

In both Characeae, there was an initial depolarization upon the hypoosmotic step, which was independent of Ca^{2+} concentration in the medium, or presence of the blockers TEA and La^{3+} (Bisson et al., 1995; Beilby and Shepherd, 1996). This response could be modeled by changing the reversal PD for the background current (see **Figure 5D**). Thus at least some of this current might flow through stretch-activated (mechano-sensitive) channels (Beilby and Shepherd, 1996; Shepherd et al., 2002).

Hypoosmotic Effect Modulation by Cell Structure and Age

Bisson et al. (1995) found that small cells (less than 10 mm in length) of *C. longifolia* regulated turgor within 60 min, while longer (and mostly older) cells took up to 3 days for full regulation. Beilby et al. (1999) and Shepherd and Beilby (1999) discovered that older *Lamprothamnium* cells developed coating of sulphated polysaccharide mucilage, identified by staining with Toluidine Blue or Alcian Blue at pH 1.0 (see **Figure 6**). With thicker mucilage the cells exhibited graded response to hypoosmotic challenge. The inflow of Ca^{2+} and streaming stoppage was not observed, but the opening of K^+ channels was retained (such as **Figure 5B**). Very mucilaginous cells exhibited only a brief depolarization with linear I/V profiles, modeled as the background current with depolarizing reversal PD (**Figure 5D**;
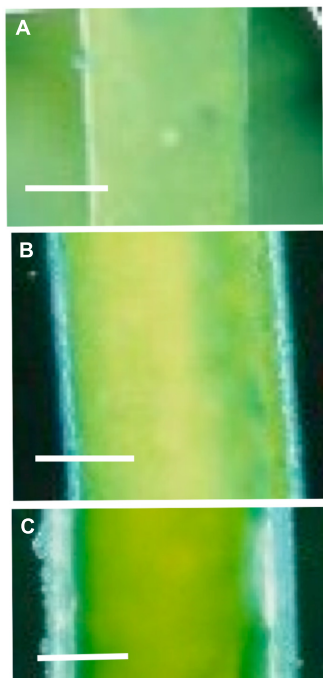

FIGURE 5 | Electrophysiology of the hypoosmotic regulation upon dilution step from 1/3 ASW to 1/6 ASW. (A) The I/V characteristics are compiled from currents fitted to cells with Cl^- current blocked by exposure to $LaCl_3$ or K^+ current blocked by TEA at times: 3 min (dark blue); 10 min (red); 15 min (magenta); 20 min (green); 30 min (blue; Beilby and Shepherd, 1996, 2001b). **(B)** The fitted Cl^- currents are shown with the same types of line as in **(A)**. These currents appear with a slight delay after hypoosmotic exposure at 10 and 15 min, and start to decline at 20 min. **(C)** The fitted K^+ currents are shown by the same types of line as in **(A)**. They appear with a greater delay at 15 min, 20 min, and 30 min. **(D)** The fitted background currents at same times as in **(A)**. Note the different scales in **(A)**, **(B)**, **(C)**, and **(D)**. While the K^+ currents are smaller than the Cl^- currents, they persist for a longer time, up to 60 min after hypoosmotic shock (the figure was adapted in color from Beilby and Casanova, 2013).

FIGURE 6 | The extracellular mucilage produced by *Lamprothamnium* plants. Cells were stained with Alcian Blue at pH 1 (Beilby et al., 1999). **(A)** Apical cell growing in ¡ ASW with mucilage ∼7 μm thick. The staining is patchy, indicating that only fraction of the mucilage is sulphated. Bar = 50 μm. **(B)** Third internode from the apex from a plant growing in full ASW. Mucilage is ∼28 μm. Bar = 100 μm. **(C)** Seventh internode of the same plant as in **(B)**, mucilage thickness is ∼43 μm. Bar = 100 μm (from Beilby and Casanova, 2013).

Shepherd et al., 1999). These cells still regulated turgor, but took 24 h or longer. Interestingly, Stento et al. (2000) were not able to find mucilage on cells of *C. longifolia* and it is possible that *Chara* genera do not produce it (Casanova, personal communication). On the other hand, Torn et al. (2014) collected six *Lamprothamnium* species from nine Australian locations and all species produced extracellular mucilage, with thickness and proportion of sulphated polysaccharides increasing with cell age, unrelated to the salinity of the environment.

After treatment of the mucilaginous cells with the heparinase enzyme, the cells responded to hypotonic shock with exaggerated depolarization, streaming stoppage and conductance increase (Shepherd and Beilby, 1999). Interestingly, the mucilage layer remained in place after heparinase treatment, but did not stain at low pH. Thus the effects of mucilage as an unstirred layer and a polyanionic layer could be separated. The removal of heparinase restored the muted response in the same cell. Young cells with no mucilage showed no change upon exposure to heparinase.

The young (fast regulating) and the old (mucilaginous and slow regulating) cells exhibited differences in sequestration of fluorochrome 6-carboxyfluorescein (6CF), which accumulated in the cytoplasm of the fast regulating cells and in the vacuole of the slow regulating cells. Beilby et al. (1999) speculated that the fast

cells have more complex vacuole structure with canalicular elements, while slow cells had large central vacuoles. Patch clamp experiments performed on cytoplasmic droplets (thought to be bound by the tonoplast membrane) from slow and fast regulating cells exhibited K^+ channels and small conductance Cl^- channels. The Cl^- channels appeared more active in slow regulating cells.
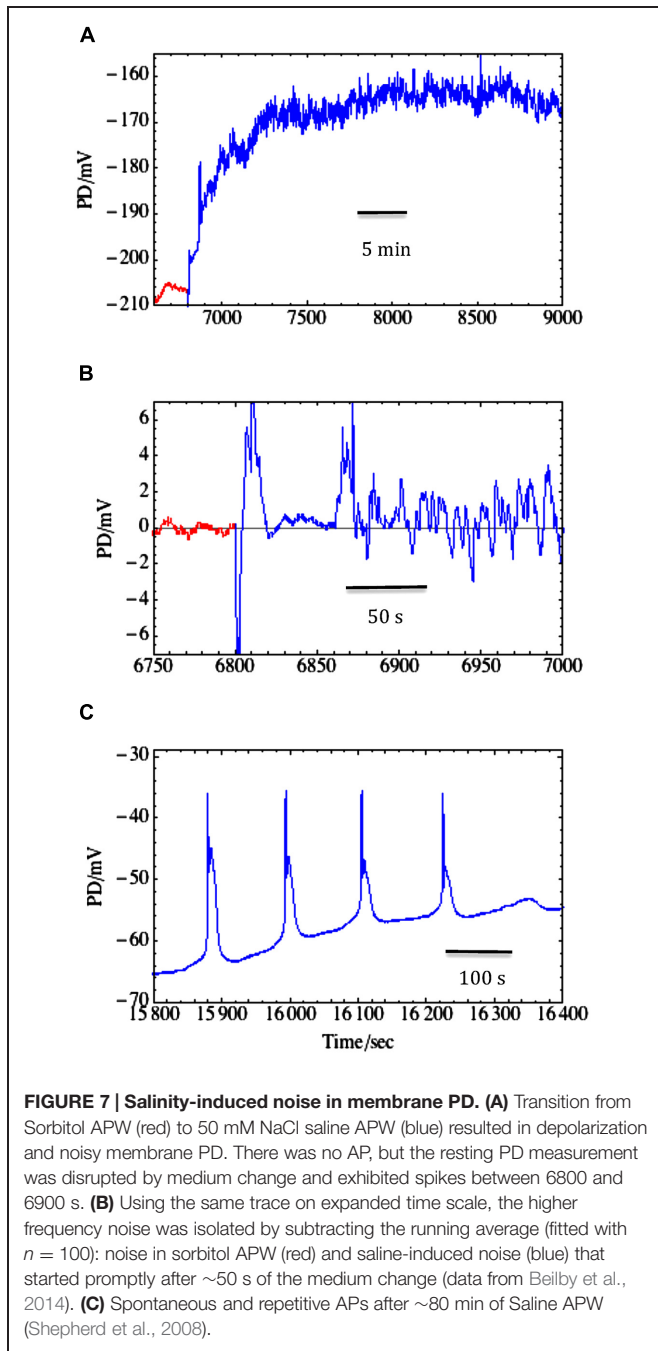
The ability of *Lamprothamnium* sp. to make extracellular sulphated polysaccharide mucilage (similar to that found in many chlorophyte marine algae) highlights another important halophytic attribute. Aquino et al. (2011) found that glycophytes of agricultural importance (*Zea mays* L., *Oryza sativa* L., and *Phaseolus vulgaris* L.) were unable to synthesize sulphated mucilage in their roots and leaves, even when challenged by increased salinity. On the other hand, salt tolerant angiosperms, such as mangroves and sea grass, and salt tolerant fern *Acrostichum aureum* contained sulphated mucilage in roots and shoots. Further, the seagrass *Ruppia maritima* L. only produced sulphated mucilage in saline media, even if the plants were supplied with abundant sulfate in the freshwater growth medium.

## Pathology of Salt Stress: Salt Sensitive Characeae

The salt sensitive *C. australis* was also exposed to the components of saline stress: sorbitol medium and saline medium of equivalent osmolarity. Shepherd et al. (2008) used 50–100 mM NaCl added to artificial pond water (APW) or 90–180 sorbitol APW. The proton pump in *Chara* cells does not respond to non-plasmolysing decrease in turgor, but can be transiently activated by an increase in Na^+ concentration if Na^+/Ca^{2+} ratio is not too high (Beilby and Shepherd, 2006a) and rapidly inactivated when Na^+/Ca^{2+} ratio increases (Shepherd et al., 2008). The increase in Ca^{2+} concentration in saline media exerts its protective influence by partially blocking NSCC channels and keeping the pump running (Bisson, 1984). The two calcium effects may be related through cytoplasmic Na^+ concentration, which may increase past some level critical to the pump. However, even at low external Na^+ (2–3 mM) the lack of Ca^{2+} caused decline of the pump activity within hours (Bisson, 1984). The inactivation of the pump brings the membrane potential to $E_{background}$, near −100 mV and at the excitation threshold. Spontaneous repetitive APs with long duration are often observed, further depleting the cell of K^+ and Cl^- (see **Figure 7C** and Shepherd et al., 2008).

The background conductance does not change upon non-plasmolysing turgor decrease (as in *Lamprothamnium*), but increases in a Ca^{2+} dependent manner in saline media (Shepherd et al., 2008). Given equivalent salt stress the background conductance is higher in *C. australis* than in *Lamprothamnium* (Beilby and Shepherd, 2006a), as low turgor was found to increase the Na^+ influx (see earlier section on Na^+ transport).

Upon transfer from sorbitol to saline medium *Chara* exhibits salinity-induced noise in the membrane PD (see **Figures 7A,B** and Al Khazaaly et al., 2009). At frequencies between 1 and 500 mHz classical noise analysis revealed $(1/f^2)$ rise of noise power as frequency falls, and a marked increase in noise

FIGURE 7 | Salinity-induced noise in membrane PD. (A) Transition from Sorbitol APW (red) to 50 mM NaCl saline APW (blue) resulted in depolarization and noisy membrane PD. There was no AP, but the resting PD measurement was disrupted by medium change and exhibited spikes between 6800 and 6900 s. **(B)** Using the same trace on expanded time scale, the higher frequency noise was isolated by subtracting the running average (fitted with $n = 100$): noise in sorbitol APW (red) and saline-induced noise (blue) that started promptly after ~50 s of the medium change (data from Beilby et al., 2014). **(C)** Spontaneous and repetitive APs after ~80 min of Saline APW (Shepherd et al., 2008).

FIGURE 8 | The response of *Chara* I/V characteristics to salinity challenge. (A) Pump-dominated profile (black) in Sorbitol APW evolved to background-dominated profile after 67 min in 50 mM NaCl Saline artificial pond water (APW; green) and to upwardly concave profile (red) after 117 min of Saline APW. The experimental data, shown as points in **(A)**, were fitted by the pump or OH^- channel models **(B)** and background current and inward rectifier models **(C)**, using same line colors as in part **(A)**. The parameters are given in caption of Figure 1 of Beilby and Al Khazaaly (2009). The dashed lines in **(B)** and **(C)** extrapolate the models beyond the range of the data. The inward rectifier channels also activate at more depolarized PDs, but the membrane PDs are more depolarized for K^+ inflow to take place.

power upon salinity challenge. Inspection of the time domain shows a continuous but random series of small rapid depolarizations followed by recovery (**Figure 7B**). As PD noise is unchanged if NaCl is exchanged for Na_2SO_4, we initially hypothesized that high Na^+ concentration activates H^+/OH^- channels. However, in recent experiments (Eremin et al., 2013) employed fluorescent probe dihydrodichlorofluorescein (DCHF) to trace reactive oxygen species (ROS) formation under strong spot illumination of *Chara* surface. The authors suggest that excess ROS formed in the chloroplasts was carried away by the cytoplasm, oxidizing either histidine or sulfhydryl (SH)
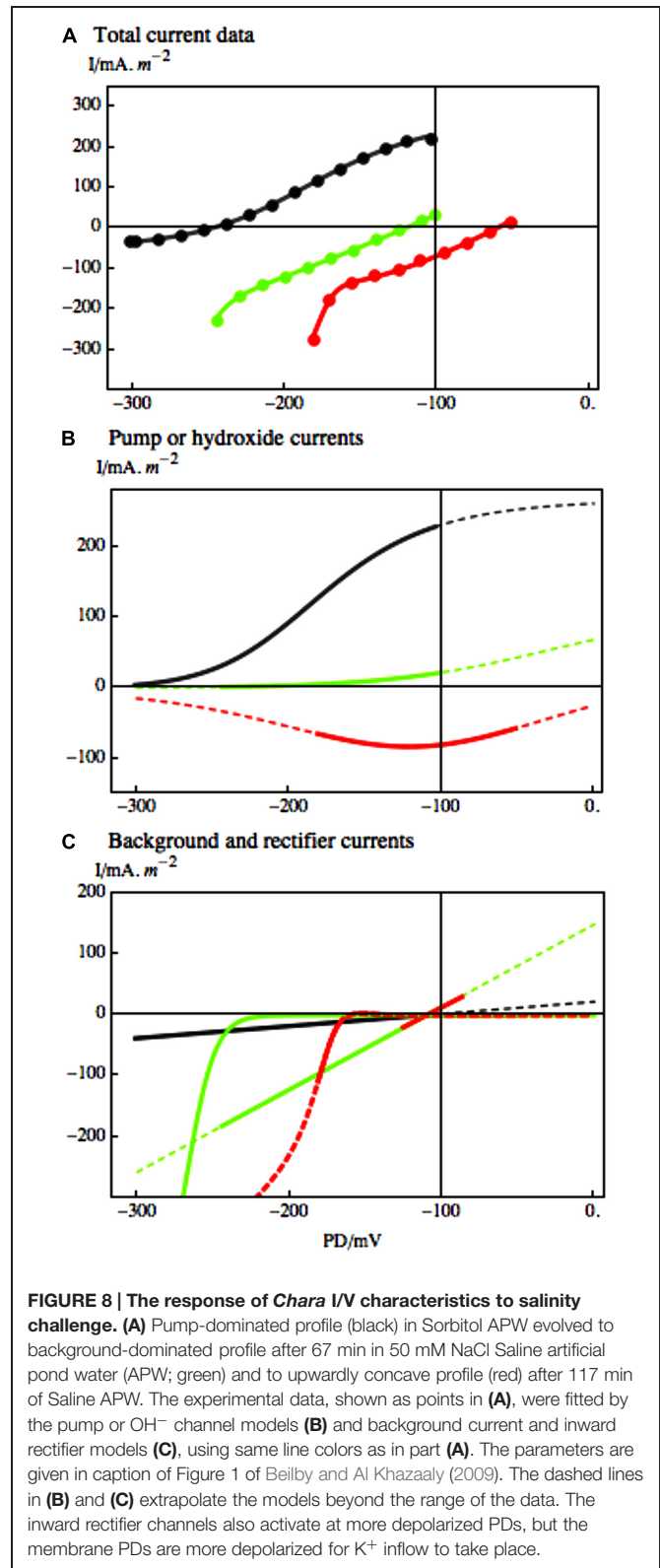
groups on transport proteins, leading to opening the H^+/OH^- channels. In the animal kingdom, the voltage-gated H^+ channels in the brain microglia are activated by H_2O_2 (Wu, 2014). Beilby
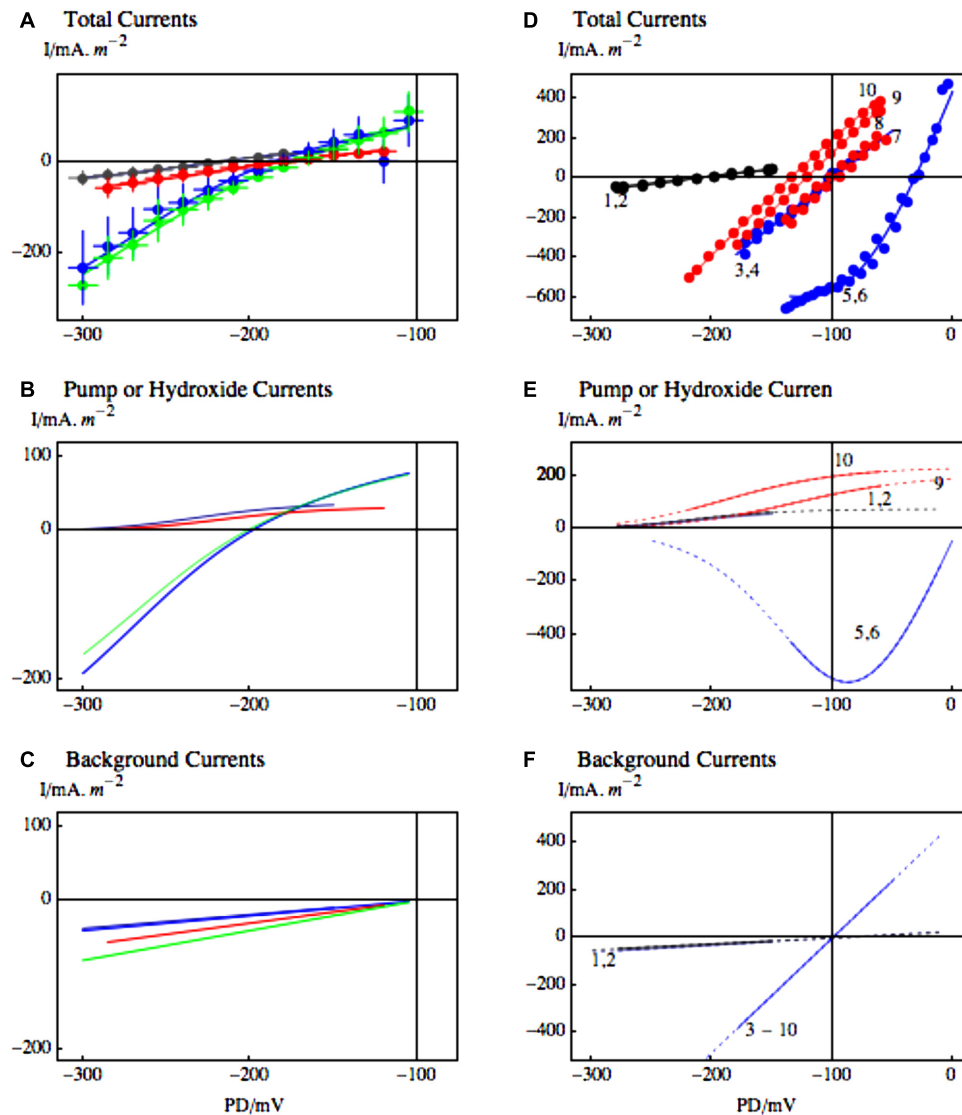
FIGURE 9 | The effect of zinc ion on the high pH state and putative H+/OH− channels at the time of salinity stress. (A) Statistics of 12 I/V profiles from 5 cells in APW (black), APW with pH increased to 11 (blue), 1.0 mM ZnCl₂ was then added to the high pH APW for average time of 36 min (red) and finally in three cells where 0.5 mM 2-mercaptoethanol (ME) replaced ZnCl₂ for average 35 min after the high pH state was inhibited (green). The data were fitted with the pump current or the OH− current **(B)**. The background current increased slightly after application of ZnCl₂ **(C)**. The fit parameters are given in

Al Khazaaly and Beilby (2012). **(D–F)** The effect of zinc ion on salinity induced I/V profiles. **(D)** The profiles 1 and 2 (black) were obtained in APW and APW with 90 mM sorbitol. After 15–30 min of APW + 50 mM NaCl, the I/V profiles 3,4 just showed the background current (blue). The resting PD then dropped further and the I/V profiles 5 and 6 were modeled with OH− channels (blue). 1.0 mM ZnCl₂ was added to the saline APW and the PD repolarized to the background current (I/Vs 7 and 8, red) and later the pump was re-activated (I/Vs 9 and 10, red). For details see Figures 2 and 4 of Al Khazaaly and Beilby (2012).

et al. (2014) were able to inhibit or postpone the saline-induced noise by presoaking the *Chara* cells in strong antioxidant mela-tonin prior to saline stress. Therefore, H+/OH− channels may be activated by an oxidative burst upon exposure to saline. Such a transient increase in ROS was observed by Li et al. (2007) upon exposing rice roots to salinity.

Once again the modeling of the I/V data allowed us to trace responses of ion transporter populations as function of expo-sure to saline. With longer exposure to high salinity, the mem-brane PD of *Chara* cells continues to depolarize toward zero,

while the noise diminishes (suggesting that progressively larger numbers of H+/OH− channels were activated – Beilby et al., 2014). The shape of the I/V characteristics changes and could be simulated by H+/OH− channels and increased background current (see **Figure 8** and Beilby and Al Khazaaly, 2009). The global opening of these channels at the time of saline stress would be disastrous for the cells, as both the negative mem-brane potential and the pH gradients between the cytoplasm, vacuole and the medium are necessary for the cell survival (**Figure 3**).

Further evidence for role of H^+/OH^- channels in the salt stress pathology is their blockage by zinc ion (Al Khazaaly and Beilby, 2012). Zinc ions are the most potent inhibitors of animal proton channels. While the permeating ion in Characeae is more likely OH^-, the channel proteins may still be closely related, as replacement of aspartate 112 by a neutral amino acid facilitated anion conduction in animal "proton" channels (DeCoursey, 2013). In Characeae the zinc ion reversibly inhibited the high pH state. The application of 0.5 mM 2-mercaptoethanol (ME) removed the zinc and restored the high pH state (**Figures 9A–C**). At the time of salt stress the depolarization to PD levels above −100 could be reversed by including 1.0 mM $ZnCl_2$ in the saline APW. Even the function of the proton pump was temporarily restored (**Figures 9D–F**). The saline noise was also inhibited by zinc ion. However, as zinc has many functions in plant tissues, further proof of H^+/OH^- channel involvement in salt stress pathology is needed.

Interestingly, Kirst and Bisson (1982) found that salt tolerant *Lamprothamnium* exposed to pH above 9.5 suffered similar fate to salt sensitive *C. australis*: the turgor dropped, concentration of Na^+ in the cell compartments increased, while concentration of K^+ and Cl^- decreased leading to cell death. We assume that high pH opened the H^+/OH^- channels, placing the *Lamprothamnium* cell in the same electrophysiological state as *Chara* in the late stages of salt stress.

Conclusions, Relevance to Higher Plants and Future Research

The salt tolerant and salt sensitive Characeae contain the same types of ion transporters (**Figure 3**), but some of these transporters respond differently to osmotic and saline stress. The salt tolerant *Lamprothamnium* and *C. longifolia* cells sense both the decrease of turgor and the increase of Na^+, and respond by pumping protons faster to maintain a negative membrane potential while keeping H^+/OH^- channels closed in the acid bands. (The pH banding phenomenon as a function of salinity is under investigation at present. pH banding was observed in *Lamprothamnium* cells acclimated to fresh water – Beilby, unpublished). The cells regulate turgor by importing more K^+, Cl^- and Na^+. Salt sensitive *C. australis* does not respond to turgor decrease, does not regulate turgor, loses the energizing pump function and negative membrane potential and undergoes spontaneous repetitive APs. The global opening of H^+/OH^- channels speeds up the irreversible decline by further decreasing the membrane PD and promoting K^+ loss through outward rectifying channels. The proton gradient powering Na^+/H^+ antiporter and $2H^+/Cl^-$ symporter is dissipated.

Is the H^+/OH^- channels and the proton pump combination just peculiar to the ancient Characeae? This complex electrophysiological motif of pH banding can be observed in higher plants: aquatic angiosperms (Prins et al., 1980), pollen tubes (Feijo et al., 1999) and, most importantly, roots of land plants (Raven, 1991). In roots the source of the current is located in the acid root sub-apical zone with the sink at the alkaline tip (Raven, 1991). The author suggests that the acid and alkaline zones facilitate acquisition of molybdenum, phosphorus and iron as well as reduction of aluminum toxicity. Protoplasts from wheat roots were found to change from pump-dominated to H^+/OH^- channel dominated state (Tyerman et al., 2001). Further, salinity induced noise was observed in wheat root protoplasts (Tyerman et al., 1997). Thus a future experiments should investigate the effect of salinity on the acid/alkaline zones of roots of both glycophytes and halophytes.

Being able to sense turgor is clearly important for salt tolerant cells. Staves et al. (1992), Shimmen (2008) suggest that it is the nodal complexes (see **Figure 1**) of the characean cells that sense difference in turgor. Future experiments are planned with node-less constructs (Beilby and Shepherd, 1989, 1991) from *Lamprothamnium* cells to find if these can still sense turgor and regulate it.

How do the turgor sensors and Na^+ sensors communicate with the proton pump? Are the proton pumps of salt tolerant and salt sensitive Characeae different? Plant H^+ ATPase is encoded by a multi-gene family. In rice a new isoform of the proton pump genetic family was observed in response to salt stress (see a review by Janicka-Russak, 2011). This isoform was similar to that found in halophyte *Suaeda maritima*. Several post-translational modifications are also suggested, involving C-terminal domain and N-terminus of the protein. Phosphorylation is regulated by 14-3-3 proteins and pump molecules might form multimeric complexes. In electrophysiological experiments the pump current can be observed directly as function of time after osmotic or salinity increase. It might be possible to probe the post-translational modifications in response to salinity stress. The imminent sequencing of *C. braunii* genome (Stefan Rensing, personal communication) will provide molecular data of proton pump structure in salt tolerant and salt sensitive Characeae.

References

Al Khazaaly, S., and Beilby, M. J. (2007). Modeling ion transporters at the time of hypertonic regulation *Lamprothamnium succinctum* (Characeae, Charophyceae). *Charophytes* 1, 28–47.

Al Khazaaly, S., and Beilby, M. J. (2012). Zinc ion blocks H^+/OH^- channels in *Chara australis*. *Plant Cell Environ.* 35, 1380–1392. doi: 10.1111/j.1365-3040.2012.02496.x

Al Khazaaly, S., Walker, N. A., Beilby, M. J., and Shepherd, V. A. (2009). Membrane potential fluctuations in *Chara australis*: a characteristic signature of high external sodium. *Eur. Biophys. J.* 39, 167–174. doi: 10.1007/s00249-009-0485-2

Allakhverdiev, S. I., and Murata, N. (2008). Salt stress inhibits photosystems II and I in cyanobacteria. *Photosynth. Res.* 98, 529–539. doi: 10.1007/s11120-008-9334-x

Allakhverdiev, S. I., Sakamoto, A., Nishiyama, Y., Inaba, M., and Murata, N. (2000). Ionic and osmotic effects of NaCl-induced inactivation of photosystems I and II in *Synechococcus* sp. *Plant Physiol.* 123, 1047–1056. doi: 10.1104/pp.123.3.1047

Amtmann, A., and Sanders, D. (1999). Mechanism of Na^+ uptake by plant cells. *Adv. Bot. Res.* 29, 75–112. doi: 10.1016/S0065-2296(08)60310-9

Aquino, R. S., Grativol, C., and Mourão, P. A. S. (2011). Rising from the sea: correlations between sulfated polysaccharides and salinity in plants. *PLoS ONE* 6:e18862. doi: 10.1371/ journal.pone.0018862

Beilby, M. J. (1984). Current-voltage characteristics of the proton pump at *Chara* plasmalemma: I. pH dependence. *J. Membr. Biol.* 81, 113–125. doi: 10.1007/BF01868976

Beilby, M. J. (1985). Potassium channels at *Chara* plasmalemma. *J. Exp. Bot.* 36, 228–239. doi: 10.1093/jxb/36.2.228

Beilby, M. J. (1986). Factors controlling the K^+ conductance in *Chara. J. Membr. Biol.* 93, 187–193. doi: 10.1007/BF01870810

Beilby, M. J. (1989). "Electrophysiology of giant algal cells," in *Methods in Enzymology*, Vol. 174, eds S. Fleischer and B. Fleischer (San Diego, CA: Academic Press), 403–443.

Beilby, M. J. (1990). Current-voltage curves for plant membrane studies: a critical analysis of the method. *J. Exp. Bot.* 41, 165–182. doi: 10.1093/jxb/41.2.165

Beilby, M. J. (2007). "Action potential in charophytes," in *International Review of Cytology*, Vol. 257, ed. K. W. Jeon (San Diego, CA: Elsevier Inc.), 43–82.

Beilby, M. J., and Al Khazaaly, S. (2009). The role of H^+/OH^- channels in salt stress response of *Chara australis. J. Membr. Biol.* 230, 21–34. doi: 10.1007/s00232-009-9182-4

Beilby, M. J., Al Khazaaly, S., and Bisson, M. A. (2014). Salinity-induced noise in membrane potential of Characeae *Chara australis*: effect of exogenous Melatonin. *J. Membr. Biol.* 248, 93–102. doi: 10.1007/s00232-014-9746-9

Beilby, M. J., and Bisson, M. A. (1992). *Chara* plasmalemma at high pH: voltage dependence of the conductance at rest and during excitation. *J. Membr. Biol.* 125, 25–39. doi: 10.1007/BF00235795

Beilby, M. J., and Bisson, M. A. (2012). "pH banding in Charophyte algae," in *Plant Electrophysiology Methods and Cell Electrophysiology*, ed. A. G. Volkov (Berlin Heidelberg: Springer-Verlag), 247–271. doi: 10.1007/978-3-642-29119-7_11

Beilby, M. J., and Casanova, M. T. (2013). *The Physiology of Characean Cells*. Berlin: Springer.

Beilby, M. J., Cherry, C. A., and Shepherd, V. A. (1999). Dual regulation response to hypertonic stress in *Lamprothamnium papulosum. Plant Cell Environ.* 22, 347–359. doi: 10.1046/j.1365-3040.1999.00406.x

Beilby, M. J., and Shepherd, V. A. (1996). Turgor regulation in *Lamprothamnium papulosum*.1. I/V analysis and pharmacological dissection of the hypotonic effect. *Plant Cell Environ.* 19, 837–847. doi: 10.1111/j.1365-3040.1996.tb00420.x

Beilby, M. J., and Shepherd, V. A. (1989). Cytoplasm-enriched fragments of *Chara*: structure and electrophysiology. *Protoplasma* 148, 150–163. doi: 10.1007/BF02079334

Beilby, M. J., and Shepherd, V. A. (1991). Reassertion of morphology and physiology in cytoplasm - enriched fragments of *Nitella. C. R. Acad. Sci.* 313, 265–271.

Beilby, M. J., and Shepherd, V. A. (2001a). Modeling the current-voltage characteristics of charophyte membranes: II. the effect of salinity on membranes of *Lamprothamnium papulosum. J. Membr. Biol.* 181, 77–89. doi: 10.1007/PL00020977

Beilby, M. J., and Shepherd, V. A. (2001b). Modeling the current–voltage characteristics of charophyte membranes III. K^+ state of *Lamprothamnium. Austr. J. Plant Physiol.* 28, 541–550. doi: 10.1071/PP01032

Beilby, M. J., and Shepherd, V. A. (2006a). The electrophysiology of salt tolerance in charophytes. *Cryptogam. Algol.* 27, 403–417.

Beilby, M. J., and Shepherd, V. A. (2006b). The characteristics of Ca^{++}-activated Cl^- channels of the salt tolerant charophyte *Lamprothamnium. Plant Cell Environ.* 29, 764–777. doi: 10.1111/j.1365-3040.2005.01437.x

Beilby, M. J., and Walker, N. A. (1981). Chloride transport in *Chara* I. Kinetics and current-voltage curves for a probable proton symport. *J. Exp. Bot.* 32, 43–54. doi: 10.1093/jxb/32.1.43

Beilby, M. J., and Walker, N. A. (1996). Modeling the current-voltage characteristics of *Chara* membranes: I. The effect of ATP and zero turgor. *J. Membr. Biol.* 149, 89–101. doi: 10.1007/s002329900010

Bisson, M. A. (1984). Calcium effects on electrogenic pump and passive permeability of the plasma membrane of *Chara corallina. J. Membr Biol.* 81, 59–67. doi: 10.1007/BF01868810

Bisson, M. A., and Bartholomew, D. (1984). Osmoregulation or turgor regulation in *Chara? Plant Physiol.* 74, 252–255. doi: 10.1104/pp.74.2.252

Bisson, M. A., Kiegle, E. A., Black, D., Kiyosawa, K., and Gerber, K. (1995). The role of calcium in turgor regulation in *Chara longifolia. Plant Cell Environ.* 18, 129–137. doi: 10.1111/j.1365-3040.1995.tb00346.x

Bisson, M. A., and Kirst, G. O. (1980a). *Lamprothamnium*, a euryhaline charophyte I. Osmotic relations and membrane potential at steady state. *J. Exp. Bot.* 31, 1223–1235. doi: 10.1093/jxb/31.5.1223

Bisson, M. A., and Kirst, G. O. (1980b). *Lamprothamnium*, a euryhaline charophyte II. time course of turgor regulation. *J. Exp. Bot.* 31, 1237–1244. doi: 10.1093/jxb/31.5.1237

Bisson, M. A., and Walker, N. A. (1980). The *Chara* plasmalemma at high pH. Electrical measurements show rapid specific passive uniport of H^+ or OH^-. *J. Membr. Biol.* 56, 1–7. doi: 10.1007/BF01869346

Blatt, M. R. (1988). Potassium-dependent, bipolar gating of K^+ channels in guard cells. *J. Membr. Biol.* 102, 235–246. doi: 10.1007/BF01925717

Boudsocq, M., and Lauriere, C. (2005). Osmotic signaling in plants. Multiple pathways mediated by emerging kinase families. *Plant Physiol.* 138, 1185–1194. doi: 10.1104/pp.105.061275

Burne, R. V., Bauld, J., and de Dekker, P. (1980). Saline lake charophytes and their geological significance. *J. Sediment. Petrol.* 50, 281–294.

Casanova, M. T. (2013). *Lamprothamnium* in Australia (Characeae, Charophyceaea). *Austr. Syst. Bot.* 26, 268–290. doi: 10.1071/SB13026

Cheeseman, J. M., and Hanson, J. B. (1979). Energy-linked potassium influx as related to cell potential in corn roots. *Plant Physiol.* 64, 842–845. doi: 10.1104/pp.64.5.842

Davenport, R., Reid, R. J., and Smith, F. A. (1996). Control of sodium influx by calcium and turgor in two charophytes differing in salinity tolerance. *Plant Cell Environ.* 19, 721–728. doi: 10.1111/j.1365-3040.1996.tb00407.x

DeCoursey, T. E. (2013). Voltage-gated proton channels: molecular biology, physiology, and pathophysiology of the Hv family. *Physiol. Rev.* 93, 599–652. doi: 10.1152/physrev.00011.2012

Demidchik, V., and Maathuis, F. M. (2007). Physiological roles of non-selective cation channels in plants: from stress to signalling and development. *New Physiol.* 175, 387–404. doi: 10.1111/j.1469-8137.2007.02128.x

Domozych, D., Ciancia, M., Fangel, J. U., Mikkelsen, M. D., Ulvskov, P., and Willats, W. G. T. (2012). The plant walls of green algae: a journey through evolution and diversity. *Front. Plant Sci.* 3:82. doi: 10.3389/fpls.2012.00082

Epstein, E. (1976). "Kinetics of ion transport and the carrier concept," in *Transport in Plants. IIB. Encyclopedia of Plant Physiology*, Vol. 2, eds U. Luttge and M. G. Pitman. (Berlin: Springer), 70–94.

Eremin, A., Bulychev, A., and Hauser, M. J. B. (2013). Cyclosis-mediated transfer of H_2O_2 elicited by localized illumination of *Chara* cells and its relevance to the formation of pH bands. *Protoplasma* 250, 1339–1349. doi: 10.1007/s00709-013-0517-8

Feijo, J., Sainhas, J., Hackett, G. R., Kunkel, J. G., and Hepler, P. K. (1999). Growing pollen tubes possess a constitutive alkaline band in the clear zone and a growth-dependent acidic tip. *J. Cell Biol.* 144, 483–496. doi: 10.1083/jcb.144.3.483

Findlay, G. P., and Hope, A. B. (1964). Ionic relations of cells of *Chara australis*: VII. The separate electrical characteristics of the plasmalemma and tonoplast. *Austr. J. Biol. Sci.* 17, 62–77.

Gradmann, D., Hansen, U.-P., Long, W. S., Slayman, C. L., and Warncke, J. (1978). Current-voltage relationship for the plasma membrane and its principal electrogenic pump in *Neurospora crassa*: I. Steady-state conditions. *J. Membr. Biol.* 39, 333–367. doi: 10.1007/BF01869898

Graham, L. E., and Gray, J. (2001). "The origin, morphology, and ecophysiology of early embryophytes: neontological and pleontological perspectives." in *Plants Invade the Land: Evolutionary and Environmental Perspectives*. eds P. G. Gensel and D. Edwards (New York, NY: Columbia University Press).

Gutknecht, J., Hastings, D. F., and Bisson, M. A. (1978). "Ion transport and turgor pressure regulation in giant algal cells," in *Membrane Transport in Biology*, Vol. III, *Transport Across Multimembrane Systems*, eds G. Giebisch, D. Tosteson, and G. Ussing (Berlin: Springer), 125–174.

Hansen, U. P., Gradmann, D., Sanders, D., and Slayman, C. L. (1981). "Interpretation of current-voltage relationships for "active" ion transport systems: I. Steady-state reaction-kinetic analysis of class-I mechanisms." *J. Membr. Biol.* 63, 165–190. doi: 10.1007/BF01870979

Hayama, T., Nakagava, S., and Tazawa, M. (1979). Membrane depolarization induced by transcellular osmosis in internodal cells of *Nitella flexilis. Protoplasma* 98, 73–90. doi: 10.1007/BF01676663

Henzler, T., and Steudle, E. (1995). Reversible closing of water channels in *Chara* internodes provides evidence for a composite transport model of the plasma membrane. *J. Exp. Bot.* 46, 199–209. doi: 10.1093/jxb/46.2.199

Henzler, T., Ye, Q., and Steudle, E. (2004). Oxidative gating of water channels (aquaporins) in *Chara* by hydroxyl radicals. *Plant Cell Environ.* 27, 1184–1195. doi: 10.1111/j.1365-3040.2004.01226.x

Hirono, C., and Mitsui, T. (1981). "The course of activation in plasmalemma of *Nitella axilliformis*," in *Nerve membrane*, eds A. G. Matsumoto and M. Kotani (Tokyo: University of Tokyo).

Hoffmann, R., and Bisson, M. A. (1986). *Chara buckelii*, a euryhaline charophyte from an unusual saline environment. I. Osmotic relations at steady state. *Can. J. Bot.* 64, 1599–1605. doi: 10.1139/b86-215

Hoffmann, R., and Bisson, M. A. (1988). The effect of divalent cations on Na$^+$ tolerance in Charophytes. I. *Chara buckelii. Plant Cell Environ.* 11, 461–472. doi: 10.1111/j.1365-3040.1988.tb01784.x

Hoffmann, R., and Bisson, M. A. (1990). *Chara buckelii*, a euryhaline charophyte from an unusual saline environment. III. Time course of turgor regulation. *Plant Physiol.* 93, 122–127. doi: 10.1104/pp.93.1.122

Hoffmann, R., Tufariello, J. M., and Bisson, M. A. (1989). Effect of divalent cations on Na$^+$ permeability of *Chara corallina* and fresh water grown *Chara buckelii. J. Exp. Bot.* 40, 875–881. doi: 10.1093/jxb/40.8.875

Hope, A. B., and Walker, N. A. (1975). *The Physiology of Giant Algal Cells*. London: Cambridge University Press.

Janicka-Russak, M. (2011). "Plant plasma memebrane H$^+$-ATPase in adaptation of plants to abiotic stresses," in *Abiotic Stress Response in Plants – Physiological, Biochemical and Genetic Perspectives*. ed. P. A. Shanker (Rijeka: INTECH), 197–218.

Kanesaki, Y., Suzuki, I., Allakhverdiev, S. I., Mikami, K., and Murata, N. (2002). Salt stress and hyperosmotic stress regulate the expression of different sets of genes in *Synechocystis* sp. PCC 6803. *Biochem. Biophys. Res. Commun.* 290, 339–348. doi: 10.1006/bbrc.2001.6201

Karol, K. G., McCourt, R. M., Cimino, M. T., and Delwiche, C. F. (2001). The closest living relatives of land plants. *Science* 294, 2351–2353. doi: 10.1126/science.1065156

Keifer, D. W., and Lucas, W. J. (1982). Potassium channels in *Chara corallina. Plant Physiol.* 69, 781–788. doi: 10.1104/pp.69.4.781

Kelman, R., Feist, M., Trewin, N. H., and Hass, H. (2004). Charophyte algae from the Rhynie chert. *Trans. R. Soc. Edinb. Earth Sci.* 94, 445–455.

Kiegle, E. A., and Bisson, M. A. (1996). Plasma membrane Na$^+$ transport in a salt-tolerant Charophyte. *Plant Physiol.* 111, 1191–1197. doi: 10.1104/pp.111.4.1191

Kirst, G. O., and Bisson, M. A. (1982). Vacuolar and cytoplasmic pH, ion composition and turgor pressure in *Lamprothamnium* as function of external pH. *Planta* 155, 287–295. doi: 10.1007/BF00429453

Kishimoto, U., and Tazawa, M. (1965). Ionic composition and electric response of *Lamprothamnium succinctum. Plant Cell Physiol.* 6, 529–536.

Li, J.-Y., Jiang, A.-L., and Zhang, W. (2007). Salt stress-induced programmed cll death in rice root tip cells. *J. Integr. Plant Biol.* 49, 481–486. doi: 10.1111/j.1744-7909.2007.00445.x

Luhring, H. (1986). Recording of single K$^+$ channels in the membrane of cytoplasmic drop of *Chara australis. Protoplasma* 133, 19–27. doi: 10.1007/BF01293183

Martin, G., Torn, K., Blindow, I., Schubert, H., Munsterhjelm, R., and Henricson, C. (2003). "Introduction to charophyte," in *Charophytes of the Baltic Sea*, Vol. 19, eds H. A. B. Schubert and I. Blindow (Königstein im Taunus: The Baltic Marine Biologists Publications), 3–14.

Oda, K. (1962). Polarized and depolarized states of the membrane in *Chara braunii*, with special reference to the transition between the two states." *Sci. Rep. Tohoku Univ. Fourth Ser. (Biology)* 28, 1–16.

Okazaki, Y., Ishigami, M., and Iwasaki, N. (2002). Temporal relationship between cytosolic free Ca^{2+} and membrane potential during hypotonic turgor regulation in a brackish water charophyte *Lamprothamnium succinctum. Plant Cell Physiol.* 43, 1027–1035. doi: 10.1093/pcp/pcf127

Okazaki, Y., and Iwasaki, N. (1992). Net efflux of Cl$^-$ during hypotonic turgor regulation upon hypotonic treatment in internodal cells of *Lamprothamnium. Plant Cell Environ.* 15, 61–70. doi: 10.1111/j.1365-3040.1992.tb01458.x

Okazaki, Y., Shimment, T., and Tazawa, M. (1984). Turgor regulation in a brackish Charophyte, *Lamprothamnium succinctum* II. Changes in K$^+$, Na$^+$ and Cl$^-$ concentrations, membrane potential and membrane resistance during turgor regulation. *Plant Cell Physiol.* 25, 573–581.

Okazaki, Y., and Tazawa, M. (1986a). Ca^{2+} antagonist nifedipine inhibits turgor regulation upon hypotonic treatment in internodal cells of *Lamprothamnium. Protoplasma* 135, 65–66. doi: 10.1007/BF01276378

Okazaki, Y., and Tazawa, M. (1986b). Involvement of calcium ion in turgor regulation upon hypotonic treatment in *Lamprothamnium succinctum. Plant Cell Environ.* 9, 185–190. doi: 10.1111/1365-3040.ep11611622

Okazaki, Y., and Tazawa, M. (1987). Increase in cytoplasmic calcium content in internodal cells of *Lamprothamnium* upon hypotonic treatment. *Plant Cell Environ.* 10, 619–621. doi: 10.1111/j.1365-3040.1987.tb01843.x

Prins, H. B. A., Snel, J. F. H., Helder, R. J., and Zanstra, P. E. (1980). Photosynthetic HCO$_3^-$ utilization and OH$^-$ excretion in aquatic angiosperms. *Plant Physiol.* 66, 818–822. doi: 10.1104/pp.66.5.818

Raven, J. A. (1987). The role of vacuoles. *New Phytol.* 106, 357–422. doi: 10.1111/j.1469-8137.1987.tb00149.x

Raven, J. A. (1991). Terrestrial rhizophytes and and H$^+$ currents circulating over at least a millimeter: an obligate relationship? *New Phytol.* 117, 177–185. doi: 10.1111/j.1469-8137.1991.tb04899.x

Raven, J. A., and Edwards, D. (2001). Roots: evolutionary origins and biogeochemical significance. *J. Exp. Bot.* 52, 381–401. doi: 10.1093/jexbot/52.suppl_1.381

Reid, R. J., Jefferies, R., and Pitman, M. G. (1984). *Lamprothamnium*, a euryhaline charophyte. IV. Membrane potential, ionic fluxes and metabolic activity during turgor adjustment. *J. Exp. Bot.* 35, 925–937. doi: 10.1093/jxb/35.6.925

Rodriguez-Navarro, A., and Rubio, F. (2006). High-affinity potassium and sodium transport systems in plants. *J. Exp. Bot.* 57, 1149–1160. doi: 10.1093/jxb/erj068

Sanders, D. (1980). The mechanism of Cl$^-$ Transport at the plasma membrane of *Chara corallina* I. Cotransport with H$^+$. *J. Membr. Biol.* 53, 129–141. doi: 10.1007/BF01870581

Sanders, D. (1981). Physiological control of chloride transport in *Chara corallina*. I. Effects of low temperature, cell turgor pressure, and anions. *Plant Physiol.* 67, 1113–1118. doi: 10.1104/pp.67.6.1113

Schutz, K., and Tyerman, S. D. (1997). Water channels in *Chara corallina. J. Exp. Bot.* 48, 1511–1518. doi: 10.1093/jexbot/48.313.1511

Shabala, S., and Lew, R. (2002). Turgor regulation in osmotically stressed *Arabidopsis* epidermal root cells. Direct support for the role of inorganic ion uptake as revealed by concurrent flux and cell turgor measurements. *Plant Physiol.* 129, 290–299. doi: 10.1104/pp.020005

Shepherd, V. A., and Beilby, M. J. (1999). The Effect of an extracellular mucilage on the response to osmotic shock in the charophyte alga *Lamprothamnium papulosum. J. Membr. Biol.* 170, 229–242. doi: 10.1007/s002329900552

Shepherd, V. A., Beilby, M. J., and Heslop, D. J. (1999). Ecophysiology of the hypotonic response in the salt-tolerant charophyte alga *Lamprothamnium papulosum. Plant. Cell Environ.* 22, 333–346. doi: 10.1046/j.1365-3040.1999.00414.x

Shepherd, V. A., Beilby, M. J., Al Khazaaly, S., and Shimmen, T. (2008). Mechano-perception in *Chara* cells: the influence of salinity and calcium on touch-activated receptor potentials, action potentials and ion transport. *Plant Cell Environ.* 31, 1575–1591. doi: 10.1111/j.1365-3040.2008.01866.x

Shepherd, V. A., Beilby, M. J., and Shimmen, T. (2002). Mechanosensory ion channels in charophyte cells: the response to touch and salinity stress. *Eur. Biophys. J.* 31, 341–355. doi: 10.1007/s00249-002-0222-6

Shimmen, T. (2008). Electrophysiological characterization of the node in *Chara corallina*: functional differentiation for wounding response. *Plant Cell Physiol.* 49, 264–272. doi: 10.1093/pcp/pcn002

Shimmen, T., and Tazawa, M. (1982). Reconstitution of cytoplasmic streaming in Characeae. *Protoplasma* 113, 127–131. doi: 10.1007/BF01282001

Smith, J. R. (1984a). The electrical properties of plant cell membranes. II. Distortion of non-linear current-voltage characteristics induced by the cable properties of *Chara. Austr. J. Plant Physiol.* 11, 211–224.

Smith, P. T. (1984b). Electrical evidence from perfused and intact cells for voltage-dependent K$^+$ channels in the plasmalemma of *Chara australis. Austr. J. Plant Physiol.* 11, 304–318.

Smith, P. T., and Walker, N. A. (1981). Studies on the perfused plasmalemma of *Chara corallina*: I. Current - voltage curves: ATP and potassium dependence. *J. Membr. Biol.* 60, 223–236. doi: 10.1007/BF01992560

Sokolik, A. I., and Yurin, V. M. (1981). Transport properties of potassium channels of the plasmalemma in *Nitella* cells at rest. *Sov. Plant Physiol.* 28, 206–212.

Sokolik, A. I., and Yurin, V. M. (1986). Potassium channels in plasmalemma of *Nitella* cells at rest. *J. Membr. Biol.* 89, 9–22. doi: 10.1007/BF01870892

Sorensen, I., Domozych, D., and Willats, W. G. T. (2010). How have plant cell walls evolved? *Plant Physiol.* 153, 366–372. doi: 10.1104/pp.110.154427

Staves, M. P., Wayne, R., and Leopold, A. C. (1992). Hydrostatic pressure mimics gravitational pressure in characean cells. *Protoplasma* 168, 141–152. doi: 10.1007/BF01666260

Stento, N. A., Gerber, N. R., Kiegle, E. A., and Bisson, M. A. (2000). Turgor regulation in the salt-tolerant alga *Chara longifolia*. *Plant Cell Environ.* 23, 629–637. doi: 10.1046/j.1365-3040.2000.00571.x

Steudle, E., and Zimmermann, U. (1974). Determination of the hydraulic conductivity and of reflection coefficients in *Nitella flexilis* by means of direct cell-turgor pressure measurements. *Biochim. Biophys. Acta* 332, 399–412. doi: 10.1016/0005-2736(74)90362-9

Tazawa, M. (1964). Studies on *Nitella* having artificial cell sap. I Replacement of the cell sap with artificial solutions. *Plant Cell Physiol.* 5, 33–43.

Tazawa, M., Kikuyama, M., and Shimmen, T. (1976). Electric characteristics and cytoplasmic streaming of Characeae cells lacking tonoplast. *Cell Struct. Funct.* 1, 165–175. doi: 10.1247/csf.1.165

Teakle, N. L., and Tyerman, S. D. (2010). Mechanisms of Cl^- transport contributing to salt tolerance. *Plant Cell Environ.* 33, 566–589. doi: 10.1111/j.1365-3040.2009.02060.x

Tester, M. (1988a). Pharmacology of K^+ channels in the plasmalemma of the green alga *Chara corallina*. *J. Membr. Biol.* 103, 159–169. doi: 10.1007/BF01870946

Tester, M. (1988b). Blockade of potassium channels in the plasmalemma of *Chara corallina* by tetraethylammonium, Ba^{2+}, Na^+ and Cs^+. *J. Membr. Biol.* 105, 77–85. doi: 10.1007/BF01871108

Tester, M. (1988c). Potassium channels in the plasmalemma of *Chara corallina* are multi-ion pores: voltage -dependent blockade by Cs^+ and anomalous permeabilities. *J. Membr. Biol.* 105, 87–94. doi: 10.1007/BF01871109

Tester, M., and Davenport, R. (2003). Na^+ tolerance and Na^+ transport in higher plants. *Ann. Bot.* 91, 503–527. doi: 10.1093/aob/mcg058

Tester, M., Beilby, M. J., and Shimmen, T. (1987). Electrical characteristics of the tonoplast of *Chara corallina*: a study using permeabilised cells. *Plant Cell Physiol.* 28, 1555–1568.

Timme, R. E., Bachvaroff, T. R., and Delwiche, C. H. F. (2012). Broad phylogenomic sampling and the sister lineage of land plants. *PLoS ONE* 7:e29696. doi: 10.1371/journal.pone.0029696

Torn, K., Beilby, M. J., Casanova, M. T., and Al Khazaaly, S. (2014). Formation of extracellular sulphated polysaccharide mucilage on the salt tolerant Characeae. *Int. Rev. Hydrobiol.* 98, 1–9.

Tyerman, S., Beilby, M. J., Whittington, J., Juswono, U., Newman, I., and Shabala, S. (2001). Oscillations in proton transport revealed from simultaneous measurements of net current and net proton fluxes from isolated root protoplasts: MIFE meets patch-clamp. *Austr. J. Plant Physiol.* 28, 591–604.

Tyerman, S., Skerrett, M., Garrill, A., Findlay, G. P., and Leigh, R. A. (1997). Pathways for the permeation of Na^+, and Cl^- into protoplasts derived from the cortex of wheat roots. *J. Exp. Bot.* 48, 459–480. doi: 10.1093/jxb/48.Special_Issue.459

Walker, N. A. (1955). Microelectrode experiments on *Nitella*. *Austr. J. Biol. Sci.* 8, 476–489. doi: 10.1071/BI9550476

Wayne, R., and Tazawa, M. (1990). Nature of the water channels in the internodal cells of *Nitellopsis*. *J. Membr. Biol.* 116, 31–39. doi: 10.1007/BF01871669

Whittington, J., and Bisson, M. A. (1994). Na^+ fluxes in *Chara* under salt stress. *J. Exp. Bot.* 45, 657–665. doi: 10.1093/jxb/45.5.657

Williams, W. D. (1998). Salinity as a determinant of the structure of biological communities in salt lakes. *Hydrobiology* 381, 191–201. doi: 10.1023/A:1003287826503

Williamson, R. E. (1975). Cytoplasmic streaming in *Chara*: a cell model activated by ATP and inhibited by cytochalasin B. *J. Cell Sci.* 17, 655–668.

Winter, U., Soulie-Marsche, I., and Kirst, G. O. (1996). Effects of salinity on turgor pressure and fertility in *Tolypella* (Characeae). *Plant Cell Environ.* 19, 869–879. doi: 10.1111/j.1365-3040.1996.tb00423.x

Wodniok, S., Brinkmann, H., Glockner, G., Heidel, A. J., Philippe, H., Melkonian, M., et al. (2011). Origin of land plants: do conjugating green algae hold the key? *BMC Evol. Biol.* 11:104–114. doi: 10.1186/1471-2148-11-104

Wu, L.-J. (2014). Voltage-gated proton channel HV1 in microglia. *Neuroscientist* 20, 599–609. doi: 10.1177/1073858413519864

Yao, X., and Bisson, M. A. (1993). Passive proton conductance is the major reason for membrane depolarization and conductance increase in *Chara buckelii* in high-salt conditions. *Plant Physiol.* 103, 197–203.

Yao, X., Bisson, M. A., and Brzezicki, L. J. (1992). ATP-driven proton pumping in two species of *Chara* differing in their salt tolerance. *Plant Cell Environ.* 15, 199–210. doi: 10.1111/j.1365-3040.1992.tb01474.x

Ye, Q., Muhr, J., and Steudle, E. (2005). A cohesion/tension model for the gating of aquaporins allows estimation of water channel pore volumes in *Chara*. *Plant Cell Environ.* 28, 525–535. doi: 10.1111/j.1365-3040.2004.01298.x

Ye, Q., Wiera, B., and Steudle, E. (2004). A cohesion/tension mechanism explains the gating of water channels (aquaporins) in *Chara* internodes by high concentration. *J. Exp. Bot.* 55, 449–461. doi: 10.1093/jxb/erh040

Conflict of Interest Statement: The author declares that the research was conducted in the absence of any commercial or financial relationships that could be construed as a potential conflict of interest.